NTNU
Norwegian University of
Science and Technology

Design of a test section to study droplet-interface coalescence under shear conditions

Santiago Martinez Santaclara

Design of a test section to study droplet-interface coalescence under shear conditions.

Santiago Martínez Santaclara

Spring 2016

NTNU

Norwegian University
of Science and Technology

Department of Energy
and Process Engineering

EPT-M-2016- 175

MASTER THESIS

for

Student
Santiago Martinez Santaclara

Spring 2016

Design of a test section to study droplet-interface coalescence under shear conditions

Background and objective

The coalescence of a water droplet with an oil interface is of relevance for gravity separators in the oil industry. Experiments and models for droplet-interface coalescence are usually developed for batch conditions. However, under real conditions in the separator, droplets are subject to shear and the coalescence phenomenon is therefore different from a batch situation. An experimental loop to study the coalescence of water droplets on an oil interface has been built.

The goal of this project will be to design the test section that will allow for the characterization of droplet-interface coalescence for different applied shear rates. The test section should allow for visual access in order to be able to observe the phenomenon with a camera.

The following tasks are to be considered:

1. Literature review on droplet-interface coalescence.
2. Design of the test section. Construction of the preliminary designs using a 3D printer.
3. Test of possible visualization and illumination setups.

2

Within 14 days of receiving the written text on the master thesis, the candidate shall submit a research plan for his project to the department.

When the thesis is evaluated, emphasis is put on processing of the results, and that they are presented in tabular and/or graphic form in a clear manner, and that they are analyzed carefully.

The thesis should be formulated as a research report with summary both in English and Norwegian, conclusion, literature references, table of contents etc. During the preparation of the text, the candidate should make an effort to produce a well-structured and easily readable report. In order to ease the evaluation of the thesis, it is important that the cross-references are correct. In the making of the report, strong emphasis should be placed on both a thorough discussion of the results and an orderly presentation.

The candidate is requested to initiate and keep close contact with his/her academic supervisor(s) throughout the working period. The candidate must follow the rules and regulations of NTNU as well as passive directions given by the Department of Energy and Process Engineering.
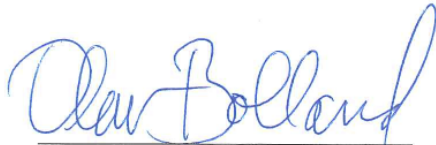
Risk assessment of the candidate's work shall be carried out according to the department's procedures. The risk assessment must be documented and included as part of the final report. Events related to the candidate's work adversely affecting the health, safety or security, must be documented and included as part of the final report. If the documentation on risk assessment represents a large number of pages, the full version is to be submitted electronically to the supervisor and an excerpt is included in the report.

Pursuant to "Regulations concerning the supplementary provisions to the technology study program/Master of Science" at NTNU §20, the Department reserves the permission to utilize all the results and data for teaching and research purposes as well as in future publications.

The final report is to be submitted digitally in DAIM. An executive summary of the thesis including title, student's name, supervisor's name, year, department name, and NTNU's logo and name, shall be submitted to the department as a separate pdf file. Based on an agreement with the supervisor, the final report and other material and documents may be given to the supervisor in digital format.

☒ Work to be done in lab (Thermal engineering lab)
☐ Field work

Department of Energy and Process Engineering, 13. January 2016

Olav Bolland
Department Head

Maria Fernandino
Academic Supervisor

Research Advisor: Carlos A. Dorao

3

I

Preface

This thesis is the result of my work performed as an exchange student at the Department of Energy and Process Engineering the spring of 2016 at the Norwegian University of Science and Technology (NTNU) in Trondheim in order to finalize my Bachelor in Energy Engineering at Universidad Politécnica de Madrid (UPM). My supervisor during this work has been María Fernandino in collaboration with Carlos A. Dorao. The topic of this master thesis is the design and construction of a test section to study droplet-interface coalescence under shear conditions related to liquid-liquid separators. The thesis has been built on both a literature study among with experimental work performed during the semester.

Abstract

Separation is a vital process in oil industries, where the mixtures separation, like the upstream gotten from oil reservoirs, differentiate the useful products. Gas-liquid separation process has been widely studied in order to optimize the quality of gas to export and later refine. However liquid-liquid separation has not been as optimized as gas-liquid separation. Nowadays liquid-liquid separators consist in a big over-dimensioned vessels, where due to the slow migration velocities and the coalescence time liquids get separate after some time. Specially in the offshore installations where space and weight play a crucial role in the design and transport of the materials is not so easy, this over-dimension of the containers can create overweight and structural issues.

In this thesis the different parts of the separation process (dynamics of droplets, and their interaction with a liquid-liquid interface) have been studied. In order to be able to conceive, design and build a facility which can simulate the processes suffered by the liquids during the separation, an extensive work in literature has been reviewed.

The goal of this work is starting from a simple circuit, design and build a test section which will allow to simulate and study the coalescence process and the droplet dynamics inside a gravity separator inducing shear by forcing flows to run in opposite directions in the presence of the other. The design was performed with 3D software and built in transparent resin in a 3D printer. A study of transparency through different post-printing processes and section designs with the addition of

crystal slides is presented. Also resistance of sections built and supports generated in a 3D printer has been performed to validate this method for experiments in the future.

The facility construction suffered modifications from the first idea due to a lack of time to perform all the components although they are included both in theory and designing part. Visualisation of the droplets was achieved with a high-speed camera over a film rail controlled by computer software. The results show the validation of the 3D prints for possible laboratory uses as the pieces are able to resist increases and reductions of flow without suffering an important pressure drop. Because of the superposition of resin layers and the aging of the resin film through the resin was rejected. A re-design of the test section was made to incorporate windows to be able to visualize and illuminate the simulation of the gravity separation process.

Contents

List of Figures

List of Tables

Glossary

A - Area

Re - Reynolds number

ρ_c - Density of the dispersed fluid

ρ_d - Density of the solution fluid

V_t^2 - Electromotive force

D - Diameter of the particle

μ_c - Continuous fluid viscosity

σ - Tension between particle and continuous fluid

We - Weber number

m - Mass of the droplet

A - Area

C_D - Drag Coefficent

d_c - Critical diameter

K_c - Proportionality factor

V_t - Terminal velocity

K_1 - Corrector factor

l/d - Non-dimensional distance between the particle and the wall

u - Velocity in the walls

U_0 - Centerline velocity

Eo - Eötvös number

Mo - Morton number

V - Volume

a - Ellipse long axis

b - Ellipse short axis

F - Collision force

$\sqrt{\frac{\epsilon}{\nu}}$ - Shear rate

ϕ - Diameter

V_{Re} - Drainage film

R_{eq} - Equivalent radius

Ca - Capillary number

Pe - Péclet number

Chapter 1

Introduction

1.1 Background

The separation process of reservoir fluids extracted from wells is a critical operation in the oil and gas industry. These fluids are mixtures of gas, oil and water that will have to be separated offshore before their transportation. This process is performed in separators, which are pressure vessels designed to divide the mixtures of gas and liquids into separate phases that are relatively free of the other fluids.

Oil extracted from reservoirs usually is composed by a large amount of water, which increased with the reservoir lifetime, where water is injected to be able to remove the oil. Refining process requires to achieve certain oil quality to be done, international requirements are a water presence in the oil less tan $0, 5\%$ [35].

Nowadays separators mainly work as gravity separators [63], with low flow rates and long residence times. The design basis of the gravity separators has been to size them to allow sufficient residence time for the settling of the liquid droplets dispersed in each phase [14]. Gravity force is the main force that accomplishes the separation, where heaviest fluids will settle at the bottom and the lightest fluid will rise to the upper part. This type of separation is very difficult due to the small density difference of water and oil, and the high viscosity of the oil, which lags water

droplets sedimentation.

Due to a lack of understanding of the sedimentation process and a lack of valid models for predicting settling times, separators are generally over-dimensioned. Residence times can be long, lasting from minutes to tens of minutes [63], and vessels are large in size to allow for a large liquid handling capacity . Separator vessels can have a diameter and length up to 3m and 25m, respectively [14]. This large dimension makes separators to be costly to purchase and install, especially in the offshore installations, where weight and space are critical design and cost parameters. Optimize these separators is of great interest for the oil industry. One of the main possibilities of improvement is to reduce the settling time required for the separation of the oil and water phases, and to acquire more accurate models of the sedimentation process that can be used to improve separator design. To accomplish this, the study of droplet dynamics with shear rate inside the separators through simulations is crucial.

Background of the problem

At the moment of this thesis just a few studies have been carried out on the behaviour of interacting water droplets in oil and neither about the influence of shear effects over the separation and coalescence processes. Knowledge regarding the settling velocity of water droplets in oil in the presence of other droplets is therefore limited.

To achieve a better understanding of separators the study of the settling velocity of drops along with the coalescence time is of importance and understanding the behaviour of a single droplet is important for the detailed knowledge of interacting drops. How a droplet interacts while moving through a fluid and in the presence of shear between liquids is useful for the determination of sedimentation velocity, coalescence and separators sizing.

The droplet size, transport properties between the phases as well as information of the droplet interface (rigid, deformable) is important when determining the sedimentation velocity [19]. The sedimentation velocity magnitude of the water droplet as it sediments through the oil differs depending on factors such as the size of the drop, as well as the properties of the oil and water and the temperature. Due to challenges related to the control of droplet size, few experimental results are available for small droplets with diameters $100m$.

In order to simulate and validate the theory performed in Chapter 2 a facility will be built. This facility (Chapter 3 and Chapter 4) is thought as two close loops (water and oil), which inside a test section simulates the separation process between liquids inside a separator through the generation of denser fluids droplets inside the lighter fluid flow. A test section has to be designed and build (Chapter 3 and Chapter 4) to simulate the processes suffered by the liquids inside the vessel. This section has to fulfil some requirements as different flow rates direction for each fluid, a transparent interface section where to record the process of the experiments and size it properly so the generated water droplets can coalesce inside of it. The facility needs to have different illumination set-ups to be able to differentiate liquids in case of similar liquids are used.

1.2   Goal of Work

The goal of this work is to design and build a facility which allows to study in the future the dependency of droplet dynamics on droplet size and changes made to the environmental conditions, in particular there will be focus on the terminal velocity and coalescence time as the temperature is changed and the influence of shear between liquids in the separation process.

To achieve this goal, it will be necessary to design and build a test section for the simulation and study of the dynamics of the sedimentation of water droplets and droplet-interface coalescence in model oil in 2D. This test section will be part of

a facility in the laboratory which consists in a close loop that generates the conditions liquids are exposed to in the separation process inside gravity separators. The objective of the experimental study in the test section is to be able to determine and record and study the terminal velocity and coalescence of water droplets falling in oil in the presence of shear between liquid interfaces. Droplets will be released over a water flow in a chimney on the test section and filmed to validate the design, study the filming process and to calibrate the system with different flow rates.

Different designs and models will be used to evaluate the viability of 3D printers to build valid pieces for the laboratory as well as transparency studies of the resin applying different treatments to the prints. Cristal slides will be attached to the walls with silicone to film through the test section and to illuminate with LED lights.

1.3   Scope of work

The theoretical background is focused on terminal velocity and coalescence process, providing a wide state of knowledge in previous experiments. The design and construction of the test section will allow future students to perform experimental analysis in the liquid-liquid separation, specifically in the droplet interface coalescence and in the terminal velocity. The study of transparency and possible applications of the 3D printer in the laboratory lay a foundation to new facility conception saving time and getting flexibility for prototypes and finally models. Experiments visualizing droplets in water will be performed in order to evaluate illumination and visualization set-ups.

1.4   Report structure

The structure of the report is explained in this section and also a short description of the content of each chapter. The dynamics of free falling liquid droplets and droplet-interface coalescence is explained in Chapter 2. Along with a short introduc-

tion, this chapter contains theory about gravity separation, terminal velocity and coalescence of rigid and deformable droplets. Among the theory there are references to previous models and studies on droplet dynamics and droplet-droplet coalescence time. In Chapter 3 a brief explanation of a possible procedure for the future droplet generation is presented. Chapter 4 shows the conception and method of design for the test section for the experimental facility. There is also a presentation of the software and printing tools. Chapter 5 presents the printing process of the test section along with the different post-printing processes applied to the pieces to improve its transparency and the conclusions and decisions about it. In this chapter the set-up of the experimental facility is presented too, with a detailed inventory of the pieces of the facility and of the auxiliary systems to record the processes inside the test section. Experimental transparency results and calibration are presented in Chapter 6. This chapter also contains a discussion of the results obtained in the different designs and treatments. Chapter 7 presents a conclusion, with recommendations for further work.

Chapter 2

Theory

2.1 Gravity separation: Three-phase & separators

In the chemical, food, and oil industries, the process of mixtures separation, like the Upstream gotten from oil reservoirs, is a vital process.

Streams from an oil reservoir are commonly composed of gas, oil, water and some solids (sand and asphaltenes). Gravity separation is the process used to separate these elements before pumping it to its destinations. The primary stage of this separation usually is performed by horizontal cylindrical gravity settling vessels with a large liquid capacity [14]. It consists on letting the upstream in a horizontal separator enough time to get it separated. Although its importance this type of separation is not optimized. Studies have been more focused in the optimization of the gas-liquid process. Nevertheless liquid-liquid separation process has its importance. As explained in the background, after oil is separated, there are international a minimum requirements in quality of the inlet oil to the refine of a $0,5\%$ [35].

Gravity separators are pressured vessels used to perform a separation of mixed-phase stream into separated liquid and gas phases. These vessels allow obtaining both phases relatively free of each other [46]. There are two possible designs for a gravity separator: Horizontal or vertical. The main difference between both remains

in the capacity volume they are provided, being the horizontal gravity separator the bigger from both. Horizontal separators have separation acting tangentially to the stream and vertical separators have separation acting horizontally to the flow. When the gas/liquid ratio unusually high, it can be defined as "scrubber" [26].

The dimensions of these vessels normally are 3m of diameter and 25 of length. Due to the size and materials, these vessels are costly to purchase and install, specially in the platforms offshore as transport and process are more difficult and where weight and space available are critical parameters in the structure resistance [14].

Another crucial point is that normally these vessels have to handle with streams from different wells, so it is needed some flexibility to be able to handle variations in the inflow affecting composition.

All the gravity separators have some components or features in common. Extracted from [26], the most important are:

- An initial section for the primary separation of liquid and gas with an inlet diverter to separate the bulk of the liquid from the gas.

- A gravity-settling section where the gas and liquid mixture is given adequate settling time for gravity separation of the phases.

- A mist extractor at the gas outlet. The mist extractor captures small droplets entrained in the gas.

- Pressure and liquid-level controls.

2.1.1   Horizontal and vertical gravity separators

The gas/liquid stream entering the separator hits the diverter changing suddenly the momentum in the mixture. It starts the bulk separation of liquid and gas and ensures that just a residual amount of gas is carried with the liquid. The liquid phase is divided in an oil phase in the top of it and water phase in the bottom. In
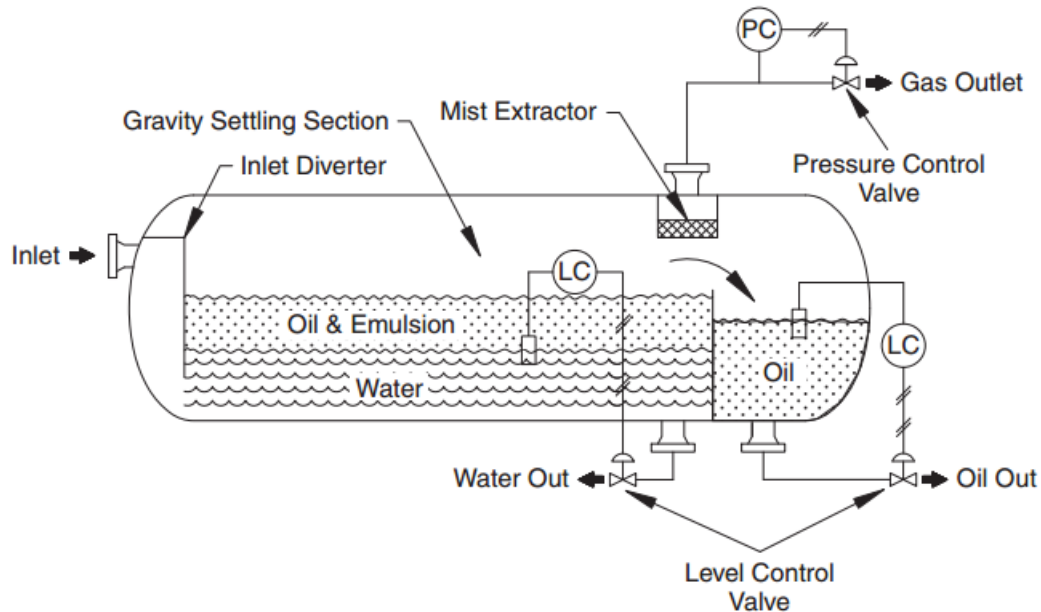
Figure 2.1: Sketch of a horizontal three-phase gravity separator [11].

this vessel section, separation between oil and watter occurs, which is called "water washing". It enhances the separation promoting the coalescence of water drops that are entrained in the oil phase when the inlet liquid mixture rise through the oil/water interface. The water washing allows an easier control over the oil/water interface as the inlet streams does not fall in the interface between gas/liquid or oil/water [11].

As it has been explained before, this process is not optimized, so what is done is to size them to allow sufficient residence time for the settling of the liquid droplets dispersed in each phase before they are removed. The level of the oil/water interface is controlled by a level controller, which is connected with a control valve upstream of the oil weir as it can be seen in Figure 2.3. Similar process is applied to the water produced in order to maintain the desired height of the interface level. Level control is less critical in vertical separators and the liquid level can fluctuate several inches without affecting the efficiency.

In the upper part, the gas flows horizontally until leave the separator through the mist extractor that is connected to a pressure vessel, which is responsible to main-

tain a constant pressure in the separator.

Although a detailed study of wall effects falls outside the scope of this thesis, is important to know some of the most important differences between horizontal and vertical separators. Normally, horizontal separators are selected when next conditions are given [46]:

- Large volumes of gas and/or liquids

- High-to-medium gas/oil ratio (GOR) streams

While vertical is often used when:

- Small flow rates of gas and/or liquids

- Very high GOR streams or when the total gas volumes are low

- Plot space is limited

- Ease of level control is desired

2.1.2   Oil-water gravity separation

The oil/water gravity separation consists in two processes, the separation of dispersed oil from the bulk water phase and the separation of dispersed water from the bulk oil phase. It is known that the oil is less dense than the water (something between 5 and 20 times), so the settling velocity of a oil droplet in water will be less than an water droplet in oil [11]. Due to this reason, manufacturers often design separators based on the settling of water droplets in oil.

In gravity separators, droplets can coalesce before settling out by gravity. These separators are based on two physical mechanisms [47]:

- Droplet coalescence: Process by which two or more droplets get in contact in order to form a bigger and unique droplet. Small droplets have to coalesce in order to be able of settling by gravity. It also describes the process of merging or fusing between droplets and a bulk of the matrix fluid.

- Droplet sedimentation: Particles in suspension have the tendency of falling through the phase and settle at the interface. It is necessary that the gravity force over droplets has to be larger than the hydrodynamic forces.

These processes can occur simultaneously or one after the other. The way processes take place depends on different factors (e.g., presence of surfactants, droplets diameter or phase viscosity.)
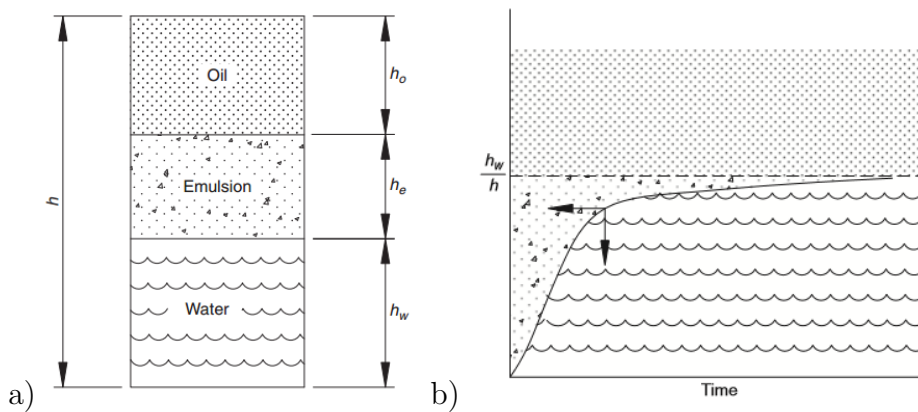
Figure 2.2: Disperser phase evolution through the time [11].

In Figure 2.2(b) it is appreciated how when the oil/water mixture enters the separator there is not a water layer in the base of the mixture. This occurs in the sedimentation zone, were water droplets have to sediment and grown in size first due to droplet-droplet coalescence. In the dense-packed zone, the droplets collect in a layer adjacent to the oil-water interface where droplet-droplet coalescence and slow sedimentation continues to occur until the water droplets finally coalesce with the bulk water phase [4].

2.2   Sedimentation: Single droplets and rigid spheres

Sedimentation is the settling of particles under the influence of gravity without net motion around particles. This process has been widely studied through the years [39].

Rigid spheres are often used as models to study the behaviour of fluid particles, but these approximations are not valid in some cases. As it has been said before, droplets motion can suffer from several mechanisms as deformation or internal circulation.
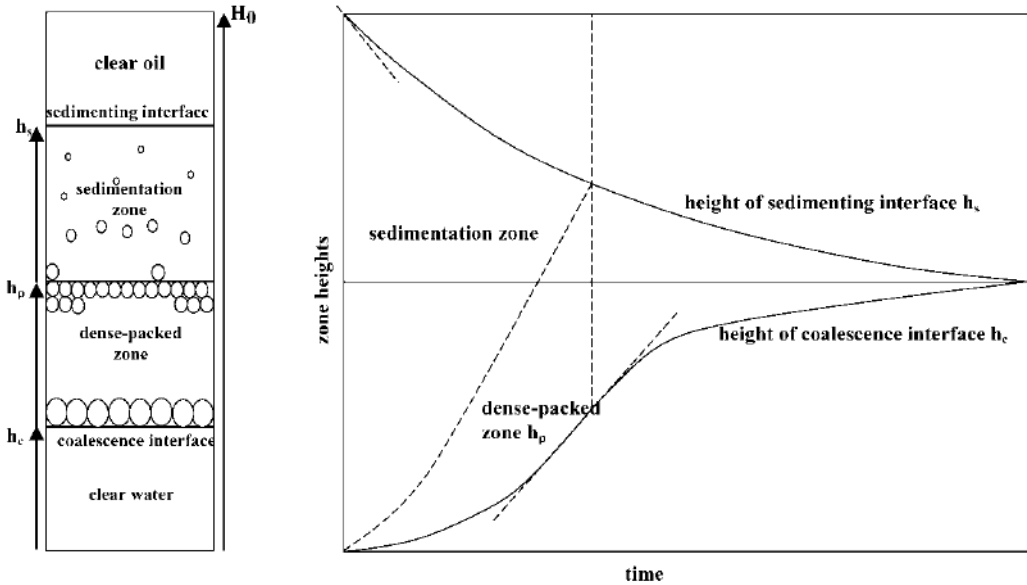
Figure 2.3: a) Schematic view of sedimentation-based model in a batch setup (left) with the sedimentation phase (top), the dense-packed zone (middle), and the coalescence interface (bottom); b) Evolution of the process through the time [11].

2.2.1 Deformation

The forces acting over it define the shape of a droplet in a steady state. Dynamic stress and static head of the exterior fluid and surface tension acting outward and in the surface are the causes of the inward forces [22]. High surface tensions between droplets at the continuous phase, it will tend to get a spherical shape [58]. The deformation a droplet can suffer is also determined by the diameter of the droplet and the Reynolds number:

11

$$Re = \frac{\rho_c \cdot V_t \cdot D}{\mu_c} \qquad (2.1)$$

Where ρ_c represents the density of the continuous fluid, V_c is the terminal velocity of the particle, D is the diameter of the particle and μ_c is the continuous fluid viscosity.

In order to characterise the shape of the droplet, several researchers have include the Weber number in this study:

$$We = \frac{\rho_c V_t^2 d}{\sigma} \qquad (2.2)$$

In Equation 2.2 σ denotes the tension between the particle and the continuous fluid. If Reynolds number is finite, for $We << 1$ droplets will tend to spherical shape. This is due to high surface tension makes low Weber number and high tensions makes droplet to tend a spherical shape as has been said before. Nevertheless for small Reynolds number, a particle in any system will remain spherical with Independence of the Weber number and the surface tension [58] [48].

2.2.2 Internal circulation

Droplets have a viscosity ratio $\left(\frac{\mu_d}{\mu_c} \right)$ finite unlike rigid spheres and internal motion in the droplet becomes important in the determination of the hydrodynamic force [52]. The tangential stress applied by the external fluid in the interface has to equalize and be opposite to the stress exerted by the internal fluid. It will lead to a relative movement of the two fluids at the interface [54]. Internal circulation causes a decrease in the boundary layer thickness of the droplet and a reduction of the flow separation angle. This makes a reduction in the drag and the terminal velocity get increased in comparison to a rigid sphere. [22].

In small droplets, internal circulation is not always present [57]. This is due to the accumulation of contaminants on the interface (as it will be explained later

in Section 2.4.2, can create big differences in the droplet behaviour [22]). If the interface is sufficiently free of contaminants, regardless the size, all droplets will have internal circulation. Water interfaces are susceptible to contaminants, specially small droplets. It is possible to eliminate internal circulation by the influence of surfactants in system with high surface tension [57].

2.2.3 Single Droplets

Precipitation of a droplet is a process in which a static droplet in a more viscous fluid will accelerate due to the gravity force until this force equals the resistance force (buoyancy and the drag force). After a time it will acquire the terminal velocity (Section 2.3) and its shape (Section 2.4.1) [22]. The motion of a spherical non-deformable particle in an incompressible Newtonian fluid is given in [54]:

$$m\frac{du}{dt} = mg\left(1 - \frac{\rho_c}{\rho_d}\right)\frac{1}{8}\pi D^2 c_D u^2 - K_{VM}\pi D^3 \rho_c \frac{du}{dt} \tag{2.3}$$

The left term on the right hand side represents the gravity-buoyancy effect while the right term is the added-mass effect due to acceleration of the Newtonian fluid around the particle. Both sides of the equation are equal to zero in s steady-state. Some of the variables have been defined already, u is the particle velocity, ρ_c is the density of the dispersed phase (particle), ρ_D the density of the Newtonian fluids, c_D the drag coefficient

There is no general expression for the terminal velocity for free-falling droplets in a fluid. This is because the drag coefficient depends on Reynolds number [57]. There are still some theoretical results obtained for the drag coefficient denominated "creeping flow regime" which is used in the Stokes' Law for rigid, spherical droplets in this regime:

$$C_{D(ST)} = \frac{24}{Re} \tag{2.4}$$

13

This equation is only valid for small Reynolds.

Laws for terminal velocity of a non-deformable droplet is defined below in Section 2.3. Classical analysis can provide a result for theoretical settling of a a single droplet in the flow regime. This analysis cannot be used for higher Reynolds due to the importance of inertial effects in this processes. As it can be expected, terminal velocity predictions can be not closer in several cases as most of the approximations are taken from little samples in comparison with the wide spectrum of situations. $Re = 0,5$ is the creeping flow limit. A deviation of 2% over Stokes Law has been found for $Re = 0,25$ and for $Re = 3,5$ deviation was settled in 17%. Above this limit settling velocity is obtained from correlations developed from experimental data [18].

2.3   Terminal velocity

When in a mixed phase of two liquids there are denser fluid droplets on the other, gravity will accelerate these droplets until the resistance (that includes drag and buoyancy) exactly balances the gravitational force [54]. Once these forces reach the equilibrium, droplets will have a constant velocity named *terminal velocity* or *settling velocity*, V_t. Usually a study of droplets shape is performed with Reynolds and Weber numbers. When droplets are very small will be considered with spherical geometry always, being unnecessary to work with Weber number.

According to bibliography, there is not a single terminal velocity Law but three different ones. For rigid spherical particles in a fluid, Perry et al. [55] provides three equations, each one for a different Reynolds number regime. Reynolds number is found following equation 2.1. For each regime exists a critical diameter for the particle. This diameter will indicates maximum diameter each law will applies:

$$d_c = K_c \left[\frac{\mu^2}{g \cdot d \cdot (\rho_s - \rho)} \right]^{1/3} \tag{2.5}$$

Where K_c is a proportionality factor distinctive for each law. These values can be calculated following equations from [55]:

Stokes' law	Intermediate law	Newton's law
$K_c = 33$	$K_c = 43,5$	$K_c = 2360$

Table 2.1: Factor distinctive for each law.

While working with a specific fluid which values to input in eq. 2.5 are known, critical diameter can be found in order to know which is the law to apply in order to get the terminal velocity. These three Laws are:

Law	Reynolds regime	Terminal velocity
Stoke's Law	0,0001$< Re <$2	$$V_t = \frac{g \cdot d^2 \cdot (\rho_s - \rho)}{18 \cdot \mu} \tag{2.6}$$
Intermediate Law	2$< Re <$500	$$V_t = \frac{0,153 g^{0,71} \cdot d^{1,14} (\rho_s - \rho)^{0,7}}{\rho^{0,29} \mu^{0,43}} \tag{2.7}$$
Newton's Law	500$< Re <$200.000	$$V_t = 1,74 \sqrt{\frac{g \cdot d \cdot (\rho_s - \rho)}{\rho}} \tag{2.8}$$

Table 2.2: Laws of settling.

Stokes' Law is applied for low Reynolds numbers and small droplets diameter. In-

termediate Law is for intermediate Reynolds and medium sized droplets, while Newton's Law is applied for high Reynolds numbers and large droplet diameter.

Most of the time droplets will not act as rigid spheres, they can experiment deformations, internal circulation and different magnitudes of the forces acting on it. Within the droplet, forces will be due to dynamical stress, internal tension and static head of the exterior fluid. External to the particle forces will be due to dynamical stress and static head of the interior fluid [30] . If droplets are considered spherical interfacial tension will be the same in all points of the surface and forces acting over the droplet will be over a radial line [22].

Wall effects

Although a detailed study of factors affecting the shape of the particle falls outside of this thesis, so that formulae given in Table 2.2 will be considered as the one to be followed, it is important to study wall effects. Proximity of the particle to the walls can cause many effects in the terminal velocity. In the equations of motion and continuity of the continuous phase boundary conditions can be changed by the effect of containing walls [57]. The shape of the droplet, its orientation and position, and the geometry of the walls are the factors that affect the droplet-wall interaction [39].

In 1983, Happel and Brenner [39] propose to include a wall correction factor K_1 to correct the drag force acting over a non-interactive rigid sphere of radious a moving axially in a circular cylindrical container of radius R_0. This factor is based on the results of a previous experiment developed in 1958 by Haberman and Sayre [64].

In figure 2.5, the solid line represents the velocity profile of a fully developed laminar flow, where l/d is the non-dimensional distance between the particle and the wall, r is the distance from the pipe centreline and R is the pipe radius [59]. This
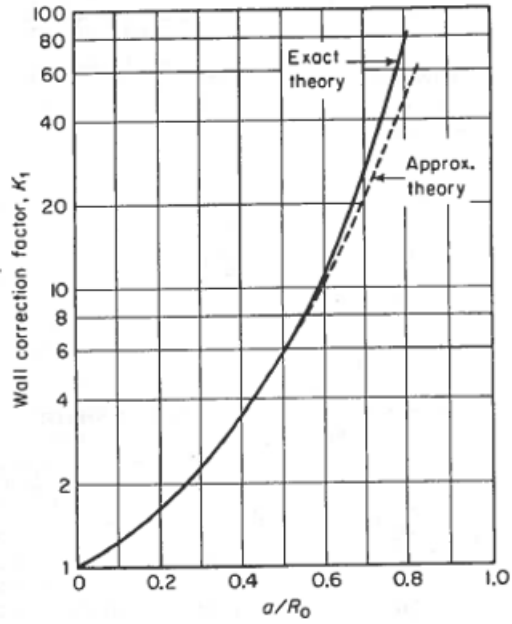
Figure 2.4: Wall correction factor K_1 from [39] extracted from results of [64].

experiment was developed in a Plexiglas pipe of 15.24 cm i.d. and 228.6 cm height in 1995.
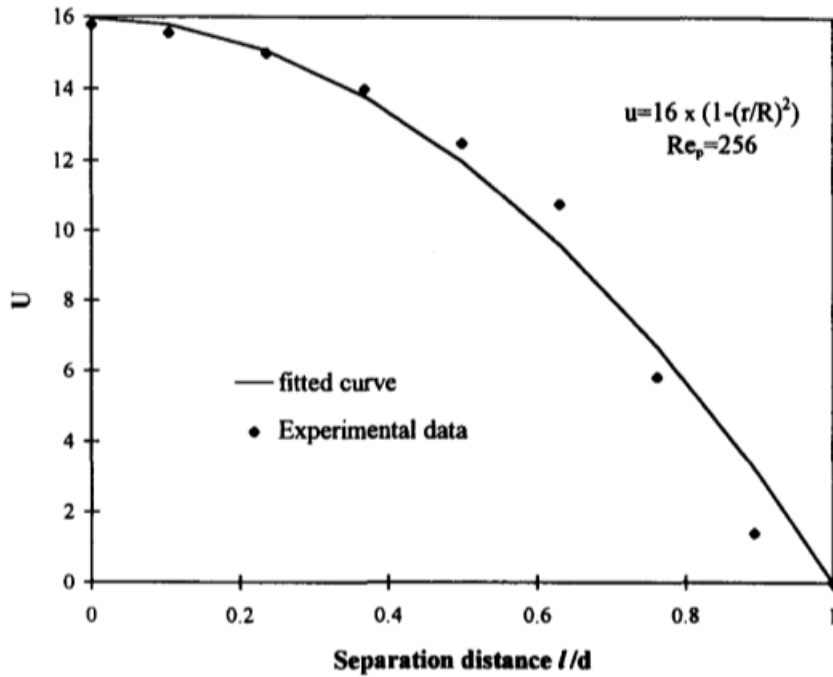
Figure 2.5: Velocity distribution along the radial direction [59].

Droplets can experience more or less drag force depending on the ratio of the droplet diameter to the diameter of the container (D/d), and the Reynolds number when subjected to the wall effect [59].

From the work of Clift, Grace and Weber in [57], equations to explain velocity in the walls for a cylindrical tube, are considered as follow:

$$u = Ui \tag{2.9}$$

The formula shown in figure 2.5, is the equivalent of eq. 2.10 from [57]:

$$u = i \left[U + U_0 \left(1 - \frac{r^2}{R^2} \right) \right] \tag{2.10}$$

Where U_0 represents the centreline velocity, i is the unit vector vertically directed upwards and U is the absolute downward velocity of the particle. As the boundary conditions are changing, it causes changes in the drag force and transfer rate. In the case of being working with fluid particles, Clift, Grace and Webber [57] make reference to an additional effect of the container walls on the particle shape. This is, the K_1 explained some lines above from [39] and [64]. So in this reference some formulas in order to calculate the factor can be found as well.

Some years later, R. C. Chen and J. L. Wu made some advances with their experimental investigation in the influence of Drag coefficient over a solid non-interactive Sphere [24]. Part of the results are shown in Figure 2.6, where C_{D0} represents the drag coefficient of the particle and $\dot{C_{D0}}$ is the diameter of the solid sphere, and l/d is the non-dimensional distance between the wall and the sphere. In the range of Reynolds that the figure is showing, it can be said that for a distance between a solid sphere to a wall higher than 2, wall effects can be neglected without making a big miscalculation in further approximations and calculations.
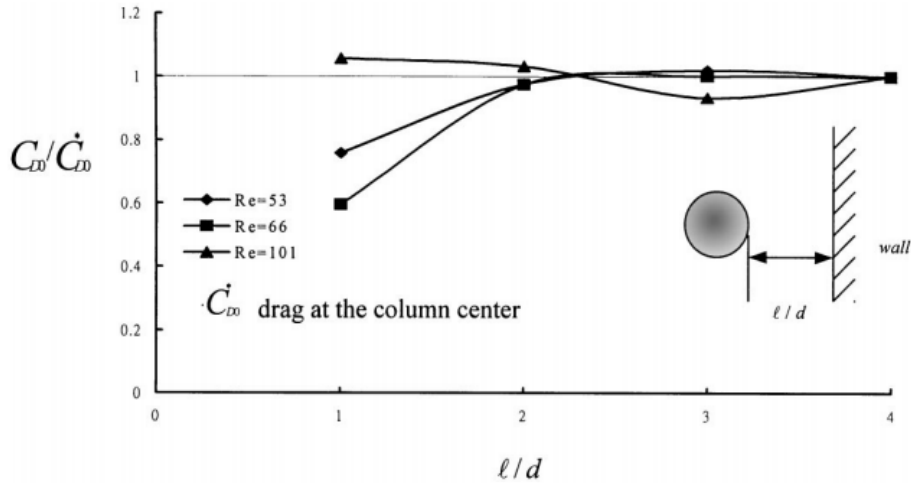
Figure 2.6: Influence of the non-dimensional distance between droplets from a wall on the drag coefficient [24].

2.3.1 Deformable droplets

If a droplet size is large enough, it will deform in the presence of external fluid fields until there is a balance between normal and shear stresses in the interface. The study of fluid particles at steady state has the advantage of the limited amount of possible shapes in comparison with solid particles because of this interfacial balance.

In 1978 Clift et al. [57] grouped under three categories the bubbles and drops free motion in an infinite media with the influence of the gravity:

a)**Spherical**: Bubbles and drops are treated as spheres if interfacial tension and/or viscous forces are much more important than inertia forces. A typical approximation is to therm a droplet as *spherical* if the difference between axes is less than 10%.

b)**Ellipsoidal**: Drops grouped in this group are oblate with a convex interface around the surface. These droplets can suffer from period dilations and wobbling motions making their shape classification difficult. Their shape may not be assumed as true ellipsoids, so fore-and-aft symmetry must not be assumed.

19

c)Spherical-cap or Ellipsoidal-cap: Drops which adopt a flat or indented bases are in this group. These drops often resemble segments cut from spheres or from oblate spheroids.

Clift et al. did a generalized graphical correlation (Figure 2.7) in terms of the Eötvös number (Eo), the Morton number (Mo) and the Reynolds number (Re):

$$Eo = \frac{g \cdot \Delta\rho \cdot d_e^2}{\sigma} \tag{2.11}$$

$$Mo = \frac{g \cdot \Delta\rho \cdot \mu^4}{\rho^2 \cdot \sigma^3} \tag{2.12}$$

$$Re = \frac{\rho \cdot U \cdot d_e}{\mu} \tag{2.13}$$
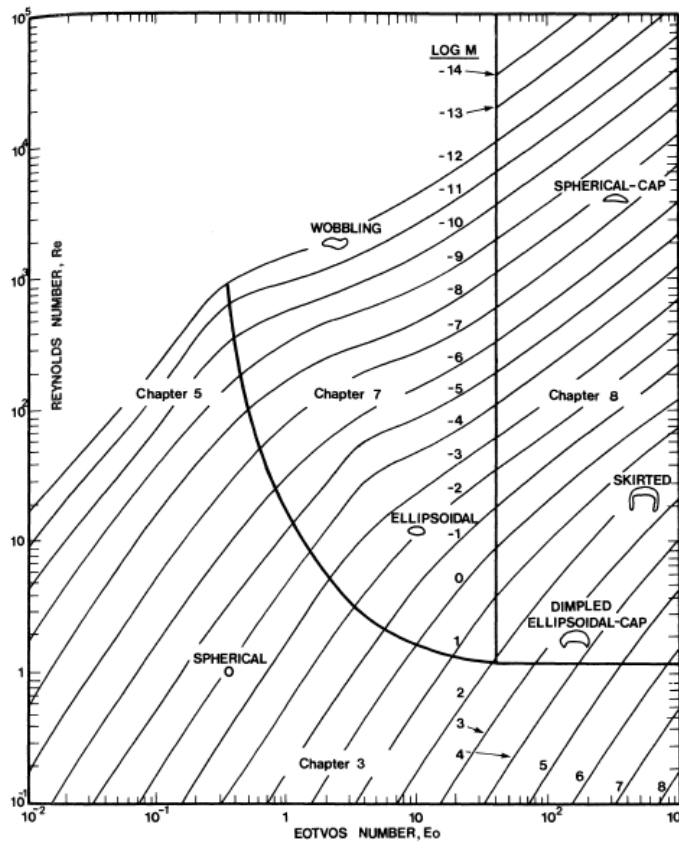
Figure 2.7: Shape regimes for bubbles and drops in unhindered gravitational motion through liquids [57].

This Figure does not apply to the extreme values of density ratio, $\gamma = \frac{\rho_p}{\rho}$ or viscosity ratio, $\kappa = \frac{\mu_p}{u}$ found for liquid drops falling through gases.

Drop deformation

Drops will flatten because of suffering a force acting upwards and downwards their surface, obtain an ellipsoidal shape. In order to obtain the equivalent diameter of the ellipse, volumes are equal. This equivalent radius is used in the plotting values of the experiments. To calculate the volume of the ellipsoidal drop the values of the semi-minor axis b and semi-major axis a are used as it can be seen in Figure 2.8.
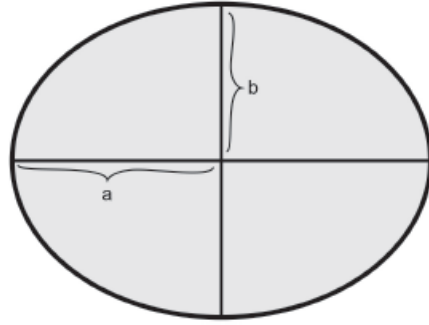
Figure 2.8: Axes of an Ellipse

$$V = \frac{4}{3}\pi r^3 = \frac{4}{3}\pi a^2 b \tag{2.14}$$

Then, applying the equation:

$$r = \sqrt[3]{a^2 b} \tag{2.15}$$

Finally the equivalent radius can be found as:

$$d = 2 \cdot r \tag{2.16}$$

2.4 Coalescence

As it has been defined in Section 2.1.2, coalescence is a process by which two or more drops get in contact in order to form a bigger and unique drop. Small drops have to coalesce in order to be able of settling faster by gravity with their weight.

The product of the collision frequency of sheared droplets and the coalescence efficiency of colliding drops determine the coalescence frequency. This is due to not every collision lead to coalescence. Droplet coalescence can be found by the coalescence efficiency of colliding droplet and the collision frequency effect [49]. This

efficiency represents the number of droplets coalescing over the total.

Droplets can be considered as non-deformable rigid spheres if droplets are very viscous compared to the continuous phase, or if droplets are very small (D<1mm) [48].

2.4.1 Film Drainage model

There are different models proposed to describe coalescence, but normally, it is explained following the film drainage model (three-stage process). This model is based in the drainage of a thin film between both surfaces of matrix fluid while it is suffering the action of gravity [40]. The coalescence time is the time from when the drop arrives at the interface and starts decelerating until it coalesces [67]. The thin film has to be drained in order to get coalescence between the elements, this drainage and rupture of the surfaces are the result of repulsive forces that stabilise the film and attractive that lead to an union [65]. Once surfaces start to be closer, Van der Waals forces can act to destabilize the film and a rupture in the surface [49].

Literature divides the film drainage model in a three-stage process:

- Approach and collide between two or more droplets, or to a bulk phase from a large distance.

- Film drainage: After the collision, there is drainage of the matrix fluid (less dense fluid) trapped between interfaces, which has to be removed.

- Destabilisation and rupture of the film leading to coalescence.

Approach and collision

When the drop approaches the interface, due to the increased viscous friction in the gap between the drop and the interface, it will decelerate. The gap between the drop and its bulk, consisting of the continuous liquid (lighter liquid) trapped between the two interface, is usually termed as "film" [67].

The introduction of the critical approach velocity model in [15] and [16] mention that small approach velocities lead to high coalescence efficiency. Anyway, contact and collision is the premise of coalescence. Collisions used to be caused by the relative velocity of the droplets. Liao and Lucas established in [48] that because of several mechanisms relative motion may occur. It is assumed that these mechanisms are cumulative. For a turbulent flow, they classified at least five of these mechanisms:

- Motion induced by turbulent fluctuations in the surrounding continuous phase.

- Motion induced by mean velocity gradients in the liquid flow.

- Different droplet sedimentation velocities due to a difference in the size of the droplets.

- Bubble capture in a swirl.

- Wake interactions between droplets.

In the experimental part of this work, it can be distinguished two different situations in the lab for which these mechanism will vary its importance. The first one, which is made in static conditions, will be the difference in sedimentation velocities and wake-entrainment. Although the second experiment has dynamic conditions, as it is with low Reynolds, it will be considered the same mechanisms adding to these the velocity gradient, as shear will be induced between interfaces. In both cases thermal gradients will be considered, as there will be temperature variations. Liao thinks in [48] that the approach and collision process will nearly never be the limiting factor in determining the coalescence rate in highly concentrated water-oil emulsion as the collision frequency, due to the proximity between droplets, is considered as 1.

In the modelling of collision frequency, models assume usually a dominant mechanism due to the complexity of taking all relevant sources into account. Mathematics models are out of the scope of this thesis, but references have been taken from the work of Liao and Lucas [48].
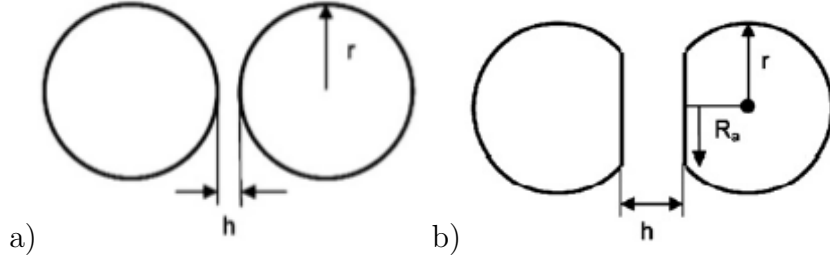
Figure 2.9: a) Non-deformable surfaces, b) Deformable surfaces [48].

If droplets do not have enough collision force, it will rebound. It is stipulated that in order for the film draining process to start, it is necessary a minimum collision duration [47]. The magnitude of this force will determine the minimum separation thickness attained during the drainage of the film. The higher the impact velocity, the higher probability that the film will drain sufficiently during the coalescence time so that the coalescence can occur [68] (Jeelani and Hartland stated that in the larger impact velocity during collisions, the larger was the force and the shorter was the time needed for the droplets to come to rest). The collision duration must be long enough so that the thin film between the droplets can drain before the droplets separate [47].

In 1991, Chesters related the collision force to an equation and another for the contact time, $t_{contact}$. For viscous fluids, [71] gives eq.2.17 and eq. 2.18:

$$F \approx 6 \cdot \phi \cdot \mu_c \cdot R^2 \cdot \sqrt{\epsilon/\nu} \tag{2.17}$$

$$t_{contact} \approx \left(\sqrt{\epsilon/\nu}\right)^{-1/2} \tag{2.18}$$

Where $\sqrt{\epsilon/\nu}$ is the shear rate. For collisions governed by inertial forces, Chesters proposed eq. 2.19 and eq.2.20:

$$F \approx \phi \cdot R_{film}^2 \cdot \left(\frac{2\sigma}{R}\right) \tag{2.19}$$

$$t_{contact} \approx \left[\left(\frac{4\rho_d}{3\rho_c} + 1 \right) \frac{\rho_c R^3}{2\sigma} \right]^{1/2} \qquad (2.20)$$

Those equations are extracted from Liao's experiments in [48].

Film drainage

The film drainage model set that in order to coalesce, the liquid film must rupture before droplets rebound (i.e. $t_{drainage} < t_{contact}$). [48] defines the drainage time as the time required to extract the liquid located in the thin film between interfaces until a critical thickness in order to lead to coalescence. Drainage time is longer than film rupture, so it will be the one to define the coalescence process [21].

During the approach the film thickness can be asymmetrical respect to the line of approach as one of the droplets can be inclined. When the process of drainage of the film starts, it can be viscous or inertial. The drainage time and the shape of the liquid film are affected by several factors such as forces over the film, physical properties or angle and velocity of approach [70].

In 1968 Lee and Hodgson defined various regimes for film drainage. These regimens explained in [56] are distinguished according to the rigidity of particles surface (In this thesis non-deformable surfaces are supposed) [48] and mobility of the contact interfaces. This mobility depends on both viscosities and the internal circulation (also affected by viscosity, contaminants and size of the droplet) and the tension gradients in the surface [5].

This drainage film can be calculated following Reynolds' equation from [62]:

$$V_{Re} = \frac{2h^3 F}{3\pi \mu_c R_{film}^4} \qquad (2.21)$$

In this equation h is the film thickness showed before in Figure 2.9, F is the interac-

tion force between the droplets, or between the droplet and the interface, and R_{film} is the radius of the film.

Non-deformable rigid spheres

The assumption of a non-deformable rigid sphere can only be done when droplets are very small (D<1mm) and very viscous in comparison with the continuous medium [47]. Although these droplets are slightly deformed, their behave is the one of a rigid sphere. In 1991 Chesters [71] derived the the film drainage time for two rigid spheres. In order to improve the approach, an equivalent radius that considers both droplets radius can be added:

$$R_{eq} = \frac{2R_1 R_2}{R_1 + R_2} \tag{2.22}$$

$$t_{drainage} = \frac{6\pi\mu_c}{F} \left(\frac{R_1 R_2}{R_1 + R_2}\right)^2 \ln\left(\frac{h_i}{h_f}\right) \tag{2.23}$$

Deformable particles

In most applications where large bubbles exist, the deformation of bubble surface during the collision has to be considered. Inside deformable particles, it is needed to differentiate between three different models [47]:

(a) Immobile interfaces.

(b) Partially mobiles interface.

(c) Fully mobile interfaces.

The parallel model is the easiest way to describe the film drainage of deformable interfaces. First developed by Frankel and Mysels in 1962 [3], it says that the surface of coalescing droplets form two parallel discs with a radius R_a as can be observed in Figure 2.10. In 1939 Derjaguin and Kussakov found dimples in the film, which implies the presence of pressure gradients in the surface. This means the impossibility of having a planar surface, as it would not withstand the pressure

gradient [25]. Pimple formation will be explained later in Section 2.4.2. Even though the dimple formation, hitherto the parallel model is the basis of the most drainage models. The mobility of the colliding interfaces will classify the regimes of drainage in the case of the deformable particles.
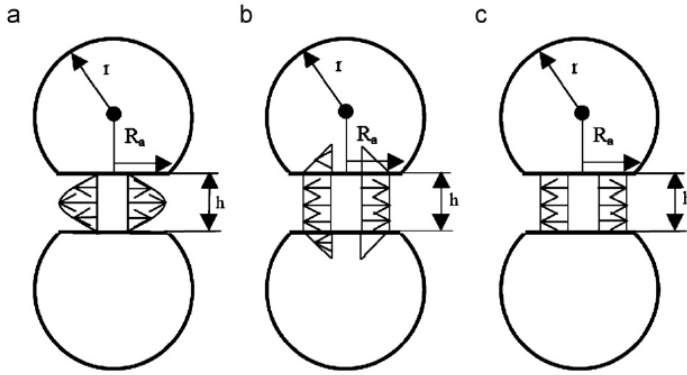
Figure 2.10: a) Immobile interface, b) Partially mobile interface, c) Fully mobile interface [41].

(a) The film drainage of the immobile interface model, (which is represented in Figure 2.10 a)), is controlled by a viscous thinning. The liquid that flows out from between the rigid surfaces is supposed to be laminar and its film velocity profile will be parabolic without slip in the boundaries conditions.

Chesters [71] bassed on a previous work of MacKay and Mason in 1963, develop a predictive equation in the case of constant forces for the drainage time, and adding the equivalent radius is:

$$t_{drainage} = \frac{3\mu_c F}{4\pi\sigma^2} \left(\frac{R_1 R_2}{R_1 + R_2} \right)^2 \left(\frac{1}{h_f^2} - \frac{1}{h_i^2} \right) \qquad (2.24)$$

This can only be applied to systems with a very high dispersed-phase viscosities or with a concentration of soluble surfactants [47].

27

(b) Many liquid-liquid systems drainage can be controlled by the motion of the film surface, the contribution or the additional flow within the film due to the pressure gradient being smaller [47]. Again, chesters [71] develop a predictive time for partially mobile interface.

$$t_{drainage} = \frac{\pi \mu_d F^{1/2}}{2(2\pi\sigma/R)^{3/2}} \left(\frac{1}{h_f} - \frac{1}{h_i} \right) \quad (2.25)$$

(c) The fully mobile interface drainage model in pure systems is the most difficult because the inertia and the viscous force control it. In 1975 Chesters developed a basis for the drainage time [69] for two equal spheres.

$$\frac{dH}{dt} = \left[\frac{\sigma}{3\mu_c R} \frac{dH}{dt} \right] exp \left(-\frac{12\mu_c t}{\rho_c R_{film}^2} \right) - \frac{\sigma}{3\mu_c R} \quad (2.26)$$

$$H = \frac{1}{2} \ln h \quad (2.27)$$

As there is no analytical solution for Equation 2.26 two limits are considered. In highly viscous liquids, the film is thinning viscously, the drainage velocity is independent of the film size and the force. Then the drainage time is settled as:

$$t_{drainage} = \frac{3\mu_c R}{2\sigma} \ln \left(\frac{h_i}{h_f} \right). \quad (2.28)$$

For the inertial thinning limit, Equation 2.26 is as shown below in Equation 2.29. Equation 2.30 is an extension made by Luao in 1993.

$$t_{drainage} = \frac{1}{2} \frac{\rho_c u_t r^2}{\sigma} \quad (2.29)$$

$$t_{drainage} = \frac{1}{2} \frac{\rho_c u_{12} d_1^2}{(1 + d_1/d_2)^2} \quad (2.30)$$

In Equation 2.29 drainage time is proportional to u_t, which is the approach velocity of the two bubbles. In Equation 2.30 is observed the dependence of the drainage time for the inertia is proportional to the velocity of approach. This is, a small drainage time.

Lee et al. [20] applying a different model (Sagert and Quinn, 1976), proposed that the inertial thinning is predominant in pure viscid fluids ($\mu_c < 10mPas$).

$$t_{drainage} = \frac{R_a}{4} \left(\frac{\rho_c d}{2\sigma} \right)^{1/2} \ln \left(\frac{h_i}{h_f} \right) \qquad (2.31)$$

Film rupture

Film rupture is considered as instantaneous. There is not a lot of studies performed in this filed. The film rupture occurs once the film is thin enough, then Van der Waals and London forces and Taylor instabilities (due to long wavelength disturbances) create instabilities in the interface. When the amplitude is the adequate this instabilities will lead to a break-up the interface leading to coalescence. If the disturbances of a wavelength are sufficiently intense can lead to coalescence too. It is not necessary all the forces to actuate in order to get coalescence [60]. This rupture can be simultaneously in two places at the same time and is observed to start at different positions.

2.4.2 Surface deformation

Although its importance does not affect small droplets as much as bigger droplets, the film between two or more objects getting approach is supposed not to have the same thickness along its frontier as Rommel et al. said in [21]. This deformation phenomena, called "$dimpling$" is mainly caused by the pressure gradient defined as Marangoni effect. The pressure suffered makes surfaces to get adapted to the new forces equilibrium. These effects is opposed by Gibbs elasticity, surface viscosity, sur-

face and bulk diffusion [7]. Marangoni effect slows and scatters the coalescence time [21].

Dimple is formed when there is no important attractive disjoining pressure and the normal viscous stress and the positive component of the disjoining pressure cannot be encountered by the capillary pressure [17]. Then, at a certain space width, surfaces will become flat and because of the viscous stress the surface will change suddenly from convex to concave shape. Both surfaces will attract each other if the disjoining pressure is negative.

Figure 2.11: Pimple and dimple formation [7].

If this pressure encounters the viscous deformation, the sum of the dynamic pressure becomes 0, and the surfaces will generate protrusions. These protrusions (opposite to the dimple) are called "*pimples*", and the gap between the dimple and the corresponding surface "*pimple thickness*" which is denoted as h_{pt} [7].
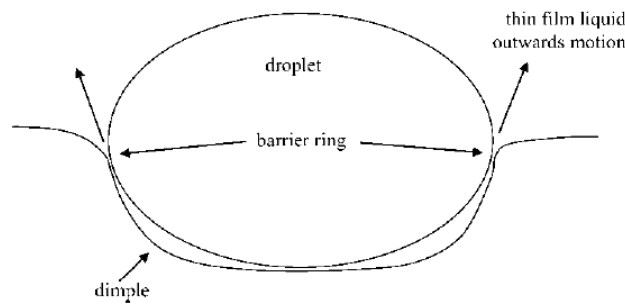
Figure 2.12: Approach of a droplet to a surface [47].

Once the liquid film at the barrier ring (figure 2.12) reaches a critical thickness, the film becomes unstable and film rupture can appear from thermal or mechanical stress [47]. The non-uniformity in the film formed between two droplets has been

observed to increase with the size of the film [53].

2.4.3   Factors affecting the coalescence

The collision force and the droplet size are not the only factors affecting the coalescence. There are several factors that contribute to stabilizing or to enhancing the process. Some of the most important are shown here:

Temperature

Interface of the films can suffer velocity gradients due to heat transfer [5]. These gradients can cause a loss in the stability of the droplets, so an increment in temperature decreases the coalescence time [38].

Droplet break-up

The coalescence ratio is affected by a previous droplet break-up before reaching the interface. This can be due to different mechanisms. Dhainaut differences in [72] some mechanism that allow this process:

- Maximum size with Rayleigh-Taylor and Kelvin-Helmholtz instabilities

- Rapid acceleration.

- Turbulent fluctuations and collisions.

- Non-uniformity in surfactant distribution.

- High shear stress.

When studying these phenomenas, Weber and Capillary numbers are used. Weber number provides an study on the ratio of inertia forces to surface tension forces:

$$We = \frac{\rho_c V_t^2 d}{\sigma} \tag{2.32}$$

Where ρ is the density of the continuous phase, V is the relative velocity between the fluid and the particle, d the droplet diameter and σ is the superficial tension.

When We ≥ 1, it means that shear forces are higher than the cohesive forces, and break-up will occur.

Capillary number provides a information about the ratio of viscous forces to surface tension:

$$Ca = \frac{\mu V}{\sigma} \qquad (2.33)$$

Where μ is the viscosity of the continuous fluid, V is the relative velocity between the fluid and the particle and σ is the superficial tension.

Capillary critical value indicates the minimum droplet size when considering the dispersive mixing of immiscible fluids. The minimum value is gotten when the fluids viscosity ratio is close to 1.If the Capillary number is small the drop will have an ellipsoidal shape due to the interfacial stress dominating. If the value of the Capillary number exceeds the critical value 25 the equilibrium shape can no longer exist, the drop becomes unstable and breaks [74].

Surfactants

The presence of surfactants in the liquids affects the drainage velocity of the thin liquid films and the hydrodynamic forces in these films as it affects the tangential mobility of the interfaces and has effects on the deformation of liquid-liquid interfaces, complicating to obtain reproducible coalescence time (for a given liquid in an interface) [38]. The presence of impurities is not necessary distributed homogeneously at the interface, so it will create interfacial tension gradients. These gradients will give rise to forces that will prolong the coalescence time [5].

The effect of the presence of surfactants on the coalescence time was studied in [40] by Hodgson and Lee. This experiment, performed with a toluene/water system. Taking as a reference point a free-surfactant system, they investigated the effect of deliberately added impurities on the coalescence time. Coalescence time was found

to be very short without the presence of surfactants in the interface and less scattered than with the presence of surfactants.

Another important factor over the coalescence time was the ageing of the interface. At some point, coalescence time increased suddenly, affecting more small droplets than large droplets. Small droplets can rest on a cohesive impurity because of the small area of the film, while larger droplets area can cover several cohesive patches impurities causing irregular thinning of the film [38].

Electro enhancement

The application of an electric field will enhance the film-thinning process. Electric fields are applied to promote the contact between droplets, this is in order to facilitate the coalescence of small droplets to get the right size and be able to precipitate due to the gravity force. It has been observed too that for a stronger electric field the contact time between droplets will decrease [13].

Electrolytes

Chen et al. found in [43] that if there is an increase in the concentration of dissolved electrolytes in systems of polar organic liquids, there will be a decrease in the coalescence time of water droplets in organic media, and an increase in the coalescence time or organic droplets in water. In previous works it was observed that when electrolytes were added to a water phase in a water/oil system, the droplet coalescence time at the interface is reduced [38] .

Vibrations and disturbances

Keelani et al. settled in [5] that coalescence times may be affected by external vibration. Taylor instabilities or an intense disturbance can lead to a film rupture causing coalescence. The pressure fluctuation on the surface due to these instabilities can include sounds and vibrations, fluid motion and interfacial turbulence [60].

Lang and Wilke in [61] found that coalescence time is very dependent on the natural vibration pattern in the environment. An intense sonic disturbance will initiate instabilities, decreasing the coalescence time. Some frequencies where found to cause droplet oscillations at the interface, increasing the film thickness and prolonging the coalescence time in comparison with cases of no disturbance present. These frequencies are lower than the calculated minimum.

Chapter 3

Experimental facility design

The main part of this project consists on the design, construction and performance of a new laboratory facility for the study of liquid-liquid separation. The idea is to simulate a gravity precipitation as in an oil vessel in the closest conditions to 2D with laminar flow. Droplets will be generated with a syringe.

3.1   Experimental facility

As is shown in Figure 3.1, the facility is a close loop composed mainly by two tanks, two pumps, a bypass, a flow meter, a DP cell and the test section. Since the loop is not pressurized, special valves are not required.

The intention is to have two liquids of different density cohabiting in the test cell. The lightest fluid (ExxolD80 or oil) will flow from the Tank 1 through the loop until the Tank 2 where it will be stored to avoid contamination of the heaviest liquid (this is, working as a gravity precipitator). Once all the first fluid is in the second Tank and impurities are removed, the recirculation pump will impulse it to Tank 1 again. The heaviest liquid (water) will be used to create the droplets that will cross the main flow inside the testing cell. Water will be stored in two different ways:

- Stored in static conditions as in a pool below the test section without opposing

the main flow.

- Flowing in a close loop counterclockwise crossing the test section and getting in contact with the main flow in the interface creating shear between fluids.

To a better understanding of how the droplet moves, the process will be filmed by a high definition camera over a film rail to follow the droplet fall inside the test section. Here remains the biggest problem in the facility design: the design of the test section, were the experiment will be carried out.
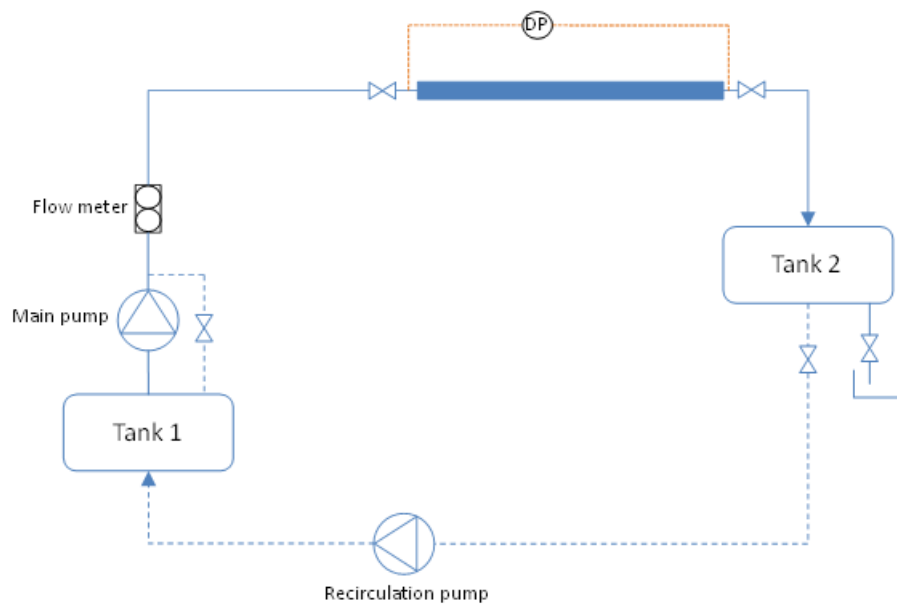

Figure 3.1: Facility sketch.

Removable test section

The test section has not been previously defined, so the effects of its design and size over the flux and the processes to measure are unknown. Therefore, several complications with the resin and its structure resistance in the printing process as other difficulties with the software design were suffered.

During this dissertation due to some issues the possibility of a Crystal-built test section was not possible because of a lack of handwork in the laboratory. Several test section designs will be studied in the 3D printer in order to get the best accuracy and similarities with glass finish.

Working fluid

In the experiment two different fluids have to be used. For the droplet generation as the denser fluid in the experiments, water was selected. The great ease of operation and an extended knowledge about its properties makes water being the profitable liquid for this operation.

As the main liquid ExxolD80 was selected.

3.2   Sketch of the test section

This section has to satisfy some pre-requisites:

- Avoid the wall effect.

- Have enough capacity for the liquid flow and make it as thin as possible (looking for 2D).

- Work in laminar flow.

- Face both liquids avoiding to mix them.

- Chimney to introduce the syringe.

In Figure 3.2 a sketch of the test section with a differentiation between what could be called "Oil section" & "Water section" can be appreciated as well as the interface
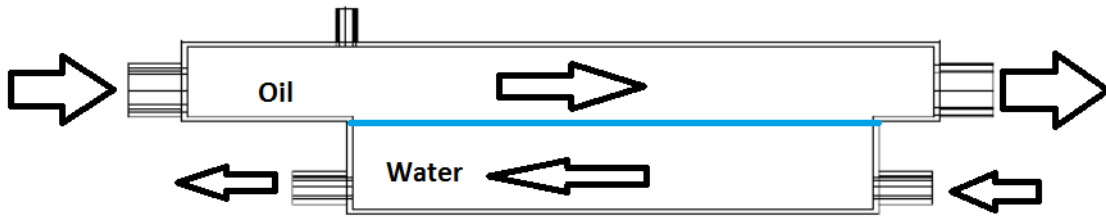
Figure 3.2: Test section sketch.

painted in blue colour.

To size the section, Reynolds number is crucial to establish the parameters in function of laminar or turbulent flow. In this case, Laminar flow is sought, which means that Reynolds number can not be bigger than 2000. Starting from a known pipe diameter $\phi = 10mm$, Reynolds in the pipe is calculated to a better understanding of what is happening before the test cell.

$$A = \frac{\pi \cdot D^2}{4} = a \cdot b \tag{3.1}$$

Equation 3.1 equals the pipe area with the area covered by the liquid in the test section. This equation will be used later to calculate Reynolds and fluid velocity inside the section.

The main pump works in a range of 30-4000 $[ml/min]$ that transformed to international system means a range from $5 \cdot 10^{-7}[m^3/s]$ to $6,67 \cdot 10^{-5}[m^3/s]$.

$$\phi_i = A \cdot v_i \tag{3.2}$$

Now, following Eq. 3.2 the velocity of the fluid through the pipe can be known. The intention is to make it slower to not miss the droplets in the current. Once velocity is calculated, Reynolds in the test section can be calculated.

$$Re = \frac{\rho_c \cdot v_t \cdot d}{\mu_c} \tag{3.3}$$

For this calculations water was used as it will be the liquid used for testing the loop. For this oil, dynamic viscosity is 5 $[cp]$, $\mu = 0,001$ and a density of 1000 $[kg/m^3]$. As

is shown in the graph [3.3], Reynolds number for the main pump variates between $16,5$ and 2223, which means that the flow rate will be laminar until a flow speed of $0,133\ [m/s]$ in the test section.

$\mathbf{D}(m)$	Density (kg/m^3)	v (m/s)	Flow rate (ml/min)	Re
0,015	1000	0,0011	30	16,5
0,015	1000	0,1482	4000	2223

Table 3.1: Reynolds variables.

In Table 3.1 variables for Reynolds calculations can be checked. Also, the kinematic viscosity is settled in $0,001\ Pa \cdot s$
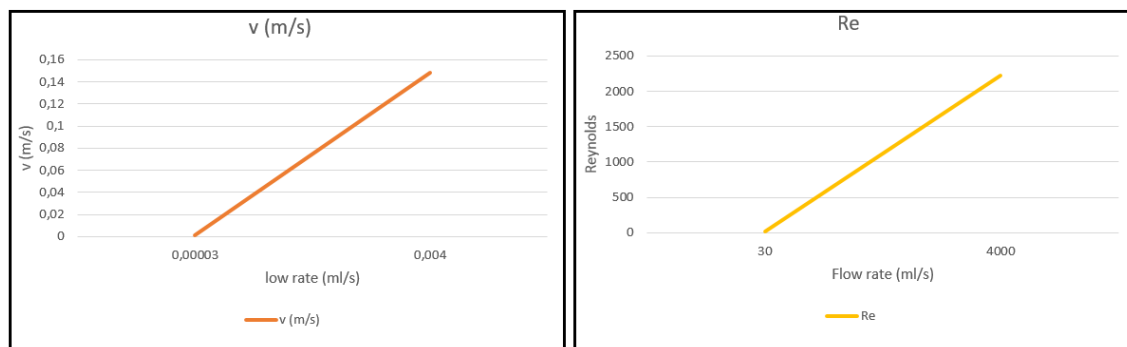

Figure 3.3: Velocity and Reynolds in the test section depending of the flow rate (ml/min).

From the table generated graphics are made. These graphics will help to control and regulate the main pump according to the experimental test.

These results shows that in order to calculate the Terminal velocity the three laws will have to be used for the different ranges indicated below in Table

Stokes' law	Intermediate law	Newton's law
0,000133 m/s	0,0333 m/s	13,333 m/s

Table 3.2: Flow speed limit for each Law.

3.3   CAD 3D design

Once dimensions are decided, the next step is to design in a 3D model the test section. For this task Autodesk Inventor ® Professional software was use. It includes options to free-form modelling, parametric and direct design automation tools and simulation tools and advanced visualization [12]. This CAD program allows the user to start from a 2D sketch, extrude it to the 3 dimensions and make modifications over it.

Test section dimensions of the first design were settled in $30x15x600$ mm for the oil section and $30x20x450$ mm for the water part of the test section. for the second design, oil section is left as is and the water section dimensions now are $30x20x500$ mm. Also the pipe connectors where settled in 15 mm each and the same diameter as the pipes that were been used in the test section construction, this is, $\phi = 12$ mm in the case of the main flow and $\phi = 8$ mm for the water circuit. On the top of the test section a chimney is located. This chimney will let to introduce a needle inside the test section to generate droplets that will be observed interacting with the different liquids and with the interface. This chimney is conceived as a cylinder of $0,5$ mm height and a diameter of $0,4$ mm.

This design is thought to be built in a real scale in crystal, but as there was no availability for making it in crystal the final test section had to be printed in a 3D printer. Due to this, the size of the section is changed to fit inside the printer parameters which are $125x125x165$ mm.

One of the possible options is to scale the 3D file in the software of the printer, but this is not a good option since there is not option for scale just an axis but all

of them. It could affect specially the plant section (see Figure 3.4) as its dimensions are very small in comparison with the length of the piece, so it would not fit in the facility.

Best option found is to remake the 3D file keeping the dimensions in the X and Y axes and resize the Z axis changing it in the first design from 600 mm and 450 mm to 135 mm and 100 mm respectively to fit in the facility. The second model will change the water section from 500 mm to 120 mm. The tube connectors were kept with same length and diameter in order to avoid problems in the connections between pipes and the test section. This could be critical for the experiment. As the piece is resized it means that the droplet will just have a $22,5\%$ of the original length to coalesce through the oil flux. If the main pump make the oil flow with a high speed through the test section the droplet could not have enough space to arrive in the water-oil interface and coalesce. A deeper scope of this will be explained later.

At first wall thickness was set in 1 mm to allow to film through the resin. Some restrictions were found as it will be explained in Section 3.5. Once the test section is designed as a solid piece, it is hollowed to allow the liquid to flow inside. To avoid the collision between the fluid in the entrance due to the thickness in the walls, the connection to the pipe mas elevated 1 mm at the entrance and exit.
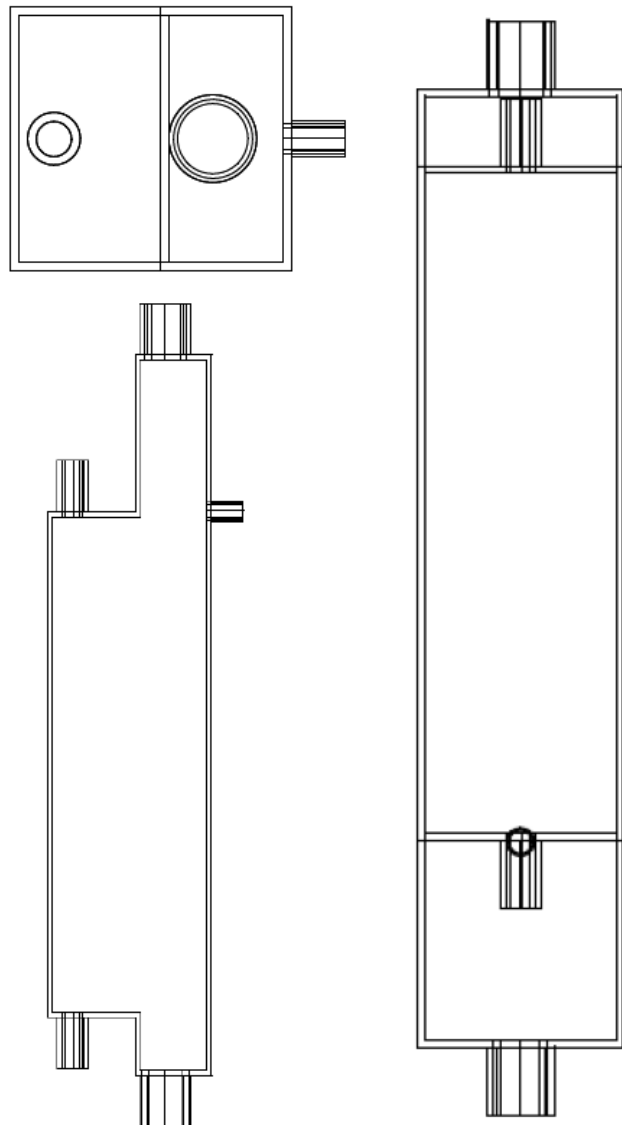
Figure 3.4: Test section planes of the first design without proportions in DWG TrueView 2016 ®: a) Plant, b) Profile, c) Elevation.
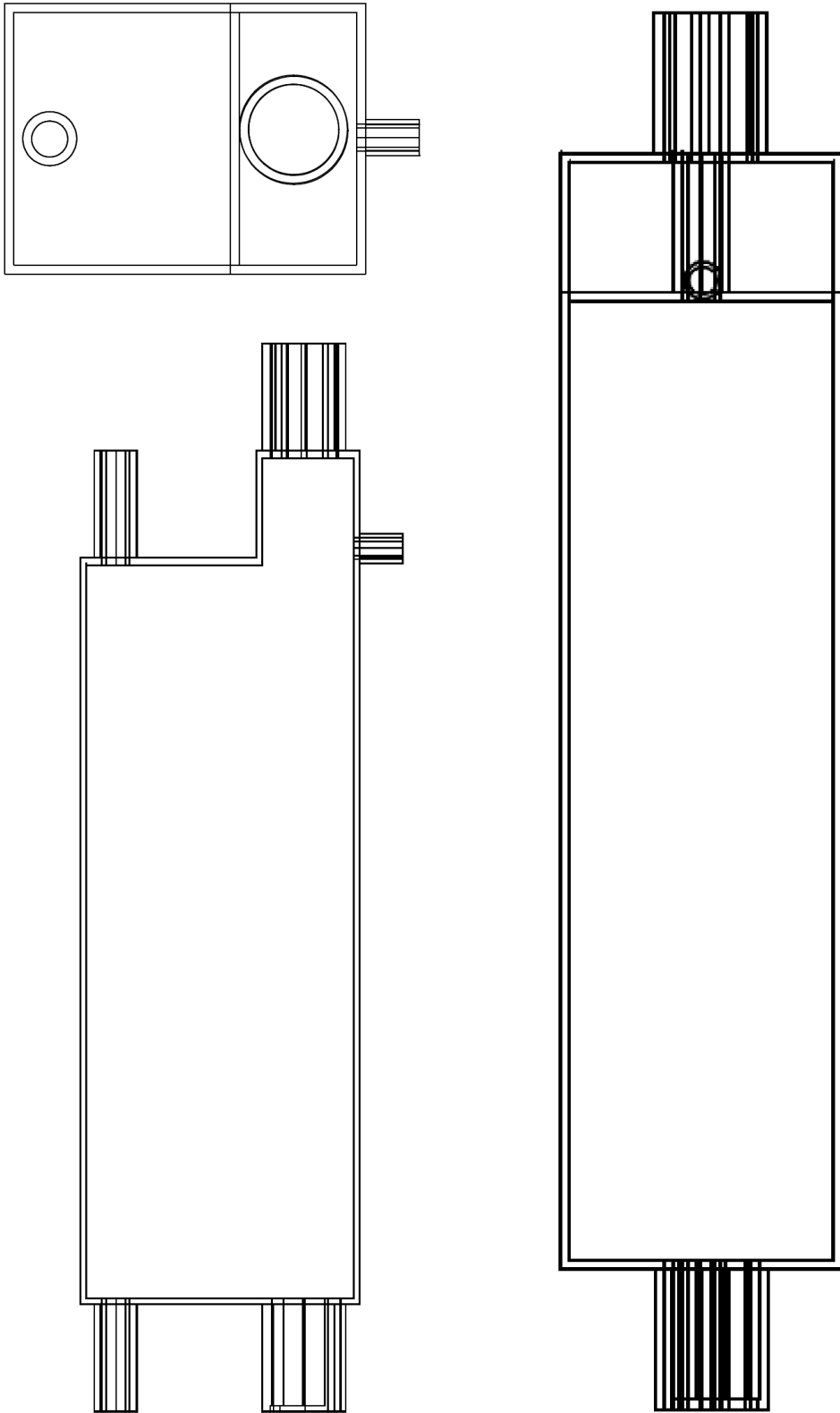
Figure 3.5: Test section planes of the second design without proportions in DWG
TrueView 2016 ®: a) Plant, b) Profile, c) Elevation.

Final proportions of both models are shown below in Table 3.3.

Model	Section	Axes			
		X	Y	Z	Z'
Design	Oil Section	30	15	600	135
I	Water Section	30	20	450	100
Design	Oil Section	30	15	600	135
II	Water Section	30	20	500	120

Table 3.3: Parameters of the test sections.

All the measurements are in millimeters, Z axis is the real measure and Z' is the scaled one to fit in the printer.

3.4 3D printer

A 3D printer provides the laboratory of a new dynamic way in the facility design and construction because of its quickness, ease of handling and accuracy transforming designed theoretical sections into material ones. These type of printers allow the laboratory personal to test several designs without large economic costs and avoiding to waste time in defective designs that do not fulfil the requirements they were made for. In some cases it does not only provides a helpful step in the way to build some elements, as also those elements can be used as permanent components in the facilities without the need of building it in other materials.

The Form 1+ is a laser 3D printer of high resolution. Its dimensions are $125x125x165$ mm and can work with different types of resins that provides the costumer of different properties for the prints. This model can print the layer thickness from 25 to 200 $microns$ and a Laser Spot Size (FWHM) of 155 $microns$ with auto-generated supports. As in this case the printer is used to research purposes that have to be filmed, the resin selected was the most transparent available, which was the *Clear Resin GPCL*02.

After have designed the test section in a 3D model, the file is exported in a .lsd file to a software compatible with the 3D printer. The manufacturer of the Form 1+ (Formlabs ®) offer a free software in its webpage [8] (PreForm Software 2.4.1). From this software plant, elevation and profile exported from Inventor were obtained as can be seen in Figure 3.4.

3.5 Manufacturing process

The designed section for the 3D printer is a big scaled model of the real design in order to fit in the printer and be able to develop the experiment in a valid conditions. The printer will overlay hundreds of tiny layers until create the test section.

One of the first factors to take into account is the type of resin the section is going to be built. It will be crucial to obtain the desired finish as it can be the transparency, flexibility or tough. In this case as the project will be focused on filming the process to a better understanding, the resin has to be as transparent as possible. *Clear Resin GPCL*02 was selected.
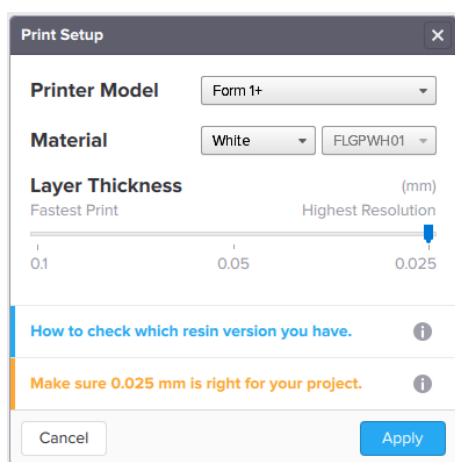
Figure 3.6: Print setup in Form-labs.

Although some design parameters selected as limits in this thesis are given as valid by the manufacturer the experience shows that they were not valid. One of these critical parameters is fixed when the Formlabs software is opened: The thickness between layers. Even though the program gives a range between $0,25\ mm$ to $2\ mm$ and the $GPCL02\ Resin$ is the unique resin that Formlabs recommends to use with $2\ mm$ the laboratory experiences during this thesis reject this thickness in the construction of medium and large sections as several prototypes where not

completed during the printing process. Three different factors are marked as possible causes of the break of some models during the test:

- Separation between layers can not be too much in order to solidify the resin and get a resilient section.

- Parameters of walls thickness settled in Inventor have to be more than 1 mm to get enough strength.

- Aging resin.

Manufactures recommend once the bottle of resin is opened to use it before 2 months or the properties of the resin can be decreased. Its cohesion and strength to solidify may be affected in the sections which supports are not well positioned since the first bottle used has been opened 4 months before this thesis.

Another of these critical parameters is the minimum supported wall thickness from the 3D design. Formlabs recommends not to input a wall thickness thinner than 0.4 mm, but the limit found during the printing part was found in 1 mm to get a certain hardness. If a thickness of 1 mm was settled the walls were easily deformable and unstable probably because of the big size and sections without supports. As it will be explained in following sections, it does not mean that the printer can not define surfaces of 0.4 mm thickness. This thickness can be included as a specific part inside a bigger one, e.g. a window frame inside the wall if necessary supports are input manually. The problem with smaller walls thickness comes when it has to provide support and strength to other components of the test section.

The solution to the problem of unsupported parts (figure 3.8) is the situation of the piece in the printer. The final printing file sent to the printer was face up so the supports could hold the piece. Also, it was found that a vertical position in the printer was not a good option. Although it allows to print a piece with a very few supports, the high number of layers needed even with a high layer thickness (around 1500 layers) which made it a very long process to print, the difficulties to print a
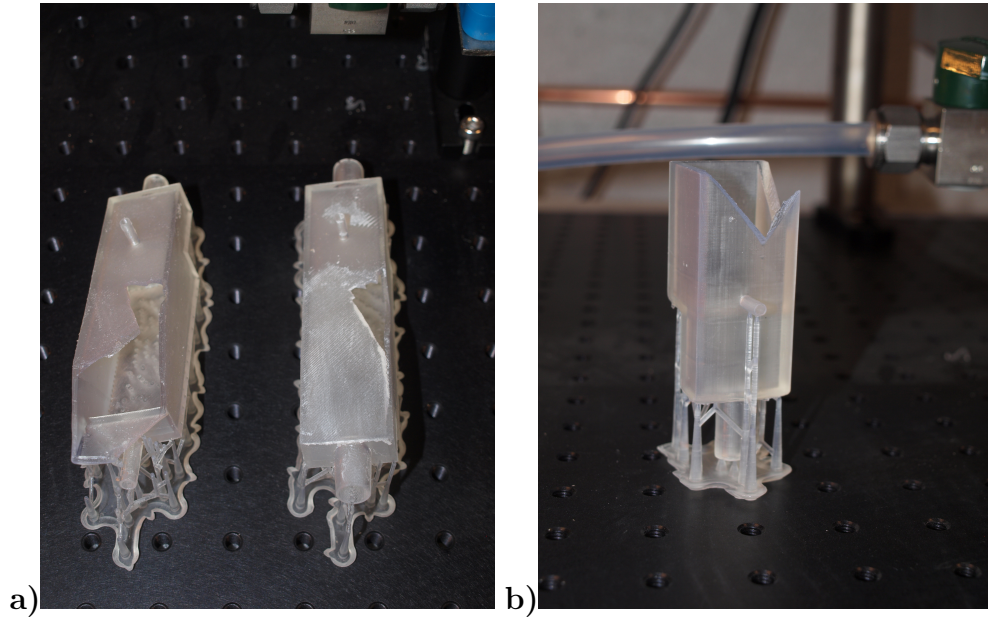
Figure 3.7: a) Uncompleted models printed with 2mm layer thickness. b) Uncompleted model printed vertically.

complete model and the bad transparency because of the verticality layers so it was rejected.

X	Y	Z
-16º	-15º	45º

Table 3.4: Axis orientation of the piece faced up in the printer.

It is necessary to study the piece tensions in the Preform Software in order to known its the viability during the printing. To support the piece is necessary to generate supports that hold the design during the printing process. It can be done manually or auto-generated by the program. There is also an option for generating supports inside the piece to shore up overhangs and other difficult geometries. This option is normally missed since there is not possible to remove the supports inside the piece. These supports will be removed later after the treatment with a solvent. After the auto-generation of supports the software gives shows regions were the printing process can be problematic due to a lack of support which is marked as red regions in the render (figure 3.8).

Before printing a checkup of the printer is needed. The most critical step found in the tuning of the printing process was the resin level. Although it is indicated to be between two marked lines in the resin tank, it is highly recommended to fill it close to the upper limit. This is due to two main reasons:

- The size of the piece, which is close to the limits of the printer.

- As working with a viscous liquid and the tank is being inclined in each layer to separate the upper support it can suffer a lack of resin in some parts momentarily, so the final piece could be not completed in some parts.

After all this settings, some of the best parameters found for this test section are shown below in Table 3.5:

Material	White FLGPWH01
Layer Thickness	0,05-0,025 mm
Wall Thickness	1-2 mm
Density Supports	0,5-0,8
Point size Supports	0,5-0,7 mm

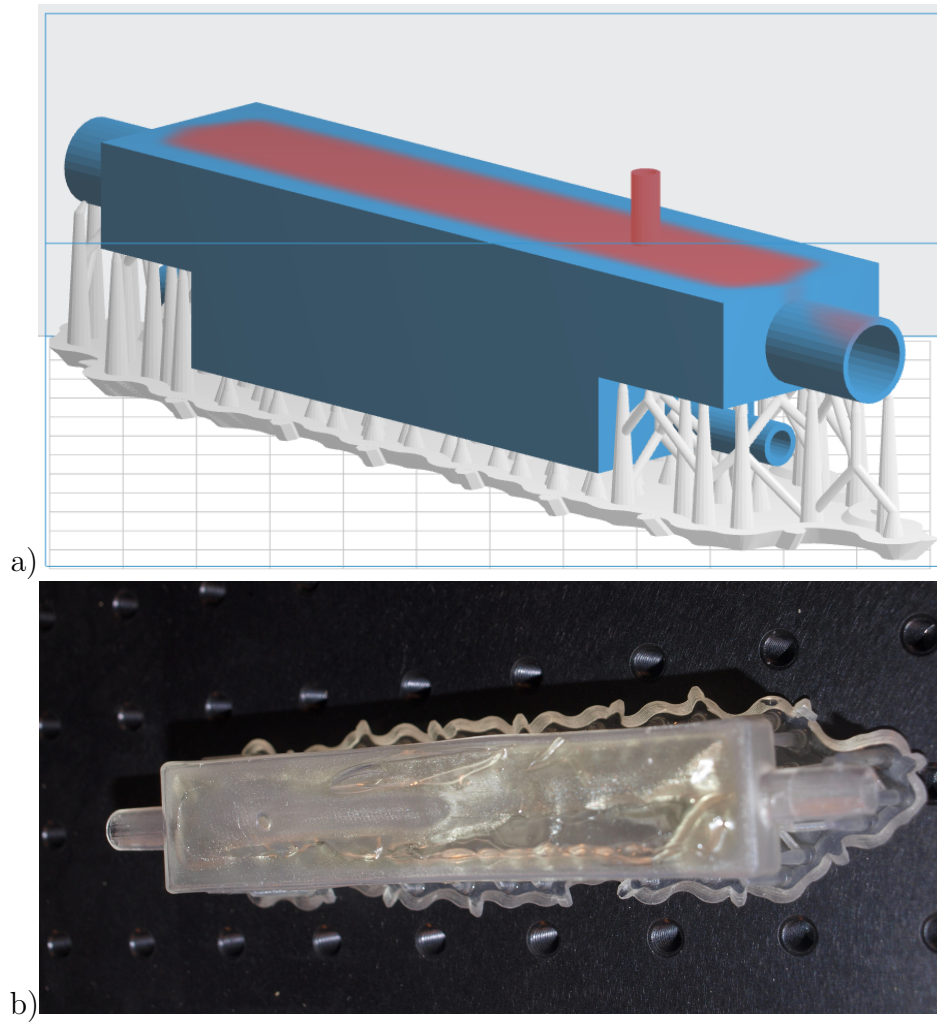Table 3.5: Range of parameters to manufacture the test section.

Figure 3.8: a) PreForm Software render study of probable critical points over the designed structure during the printing process. b) Uncompleted printed model with critical points in its upper part.

Chapter 4

Facility construction

Test section

4.1 Printed models treatment

Some unsuccessful models have been presented in previous sections as examples of possible failures during the printing process. After some test models for a first contact with the printer to know its bowels some valid models saw the light.

These first valid models where treated with different chemical processes to study their effect on the solidified resin. The reason of this study is try to get the best transparency trough the resin to be able to film behind the walls.

The manufacturer recommends to immerse the printed object some minutes in a dilution of isopropyl alcohol. It is a colorless, flammable chemical compound with a strong odor, so it will have to be stored in a hermetic box out of direct light where it will not evaporate unless it has contact with the ambient. The reason for this last process is to remove the viscous resin leftovers over the test section to weaken the supports connections to it and make their removal easier. After it is cleaned with water to remove rest of the alcohol and resin. The negative part of this process is that the resin colour gets cloudy and loses the transparency, which is the purpose
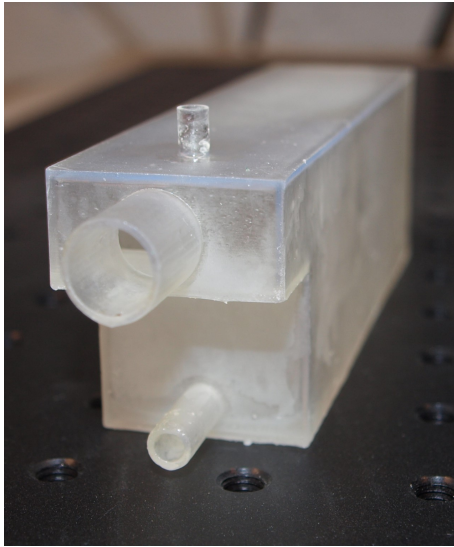
of this work.

Figure 4.1: Finish with a treatment based on isopropyl alcohol.

Formlabs' webpage offers some advices from experts to get better results in the printings. Following some of this advices to get an improved transparency, some models were treated with a polished process on a wet sandpaper of 800 grid and later with one of 1200 grid. After the polished, it was treated with an acrylic cleaner over a cork board. This method was followed with and without a previous immersion of the test section in isopropyl. The best result was gotten with the model pre-treated with isopropyl since the one just pre-treated with water was sticky because of remaining liquid resin over the section, so it gets dirty. Nonetheless the other pre-treated with alcohol was not a successful process (see Figure 4.2) as the cloudy colour of the resin did not allow to observe the inside of the test section and because of the sand paper it was scratched.
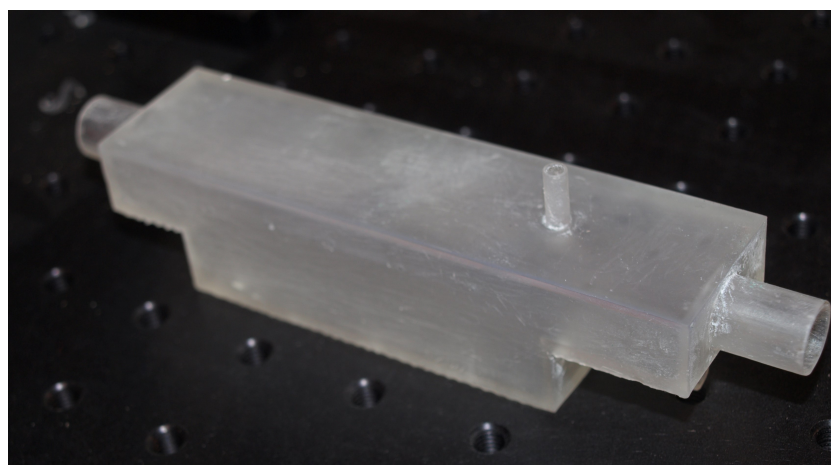
Figure 4.2: Finish following the instruction of Formlabs to improve the transparency.

From this point some home processes were tried using the available material of the lab. The first idea was to treat the test section with another alcohol which could remove the resin without removing the transparency. The alcohol selected was ethanol, an antiseptic alcohol. This process results were similar to the ones of the isopropyl, so it was rejected.

The second process thought was to clean the the test section with soap and water but the rests of resin were sticking the filaments of the sponge and the soap so neither was valid. Finally, the simplest process got the best finish: clean the test section with warm water and paper. Although the piece was remaining a little sticky it also was not loosing much transparency if keeping it in a clean space out of dust.

Figure 4.3: a) Isopropyl treatment. b) Formlabs process. c) Warm water treatment.
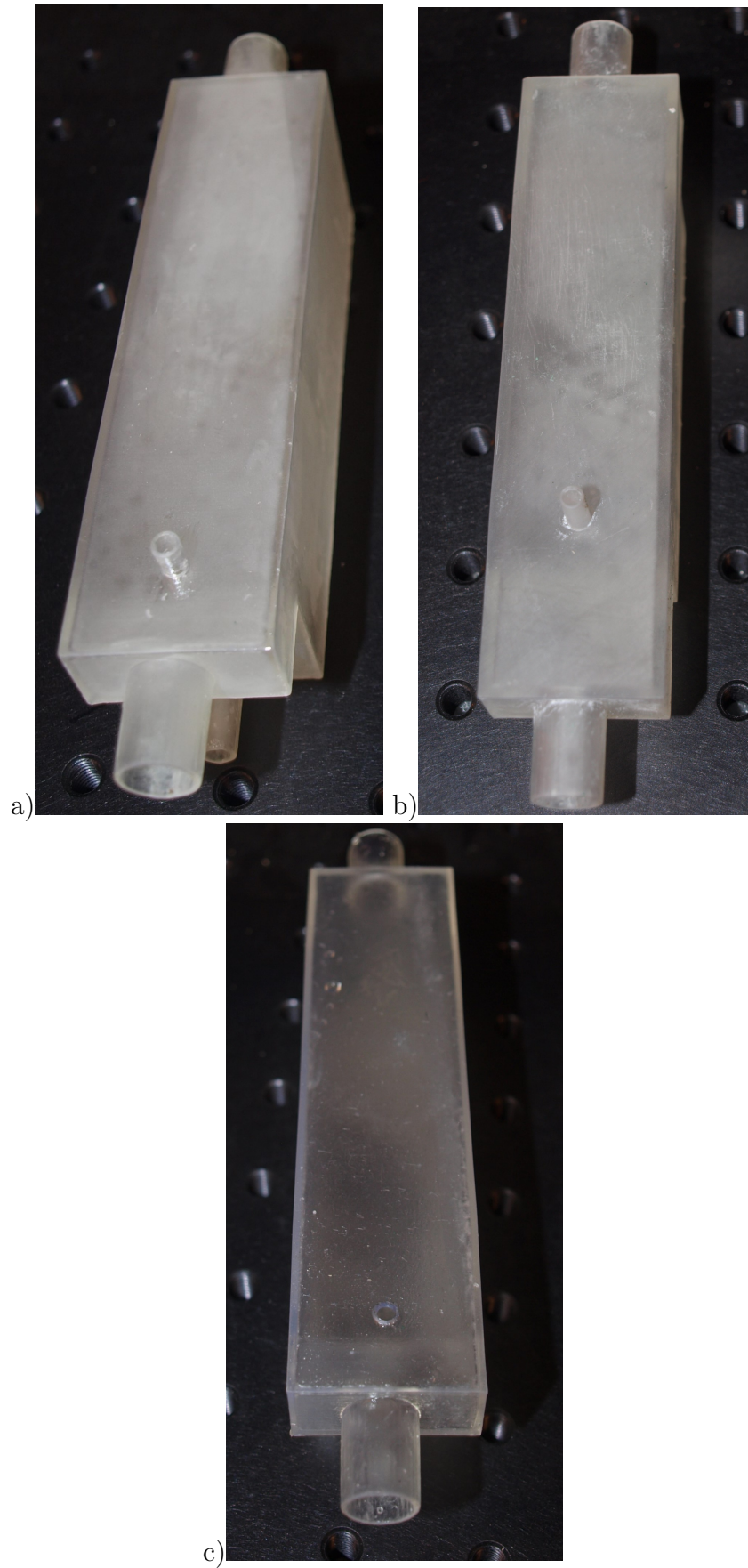
4.2 New model design

Now the situation of the project is as follows:

- The designed test section is valid for running the facility.

- The facility is not able to film the process.

Summarizing, although the design of the test section is valid, the use of resin for its construction makes it uncompleted for the requirements of filming.

In order to solve the film issues, a re-design of the test section was selected as the best option. Assuming that both models were correct in their shapes, probably with some modifications it would work. One option is to use crystal slides as those used to keep samples in good conditions to observe in the microscope as lateral windows of the test section. If the 3D printer accepts the modifications, the option of opening a window frame in both sides of the test section and later paste the crystal slides in both sides it could be possible to film the interface and the droplet sedimentation.

The idea is to open both side walls, where the slides can be fixed with some glue or silicone. One will be to film trough it and the other for illumination. To export the conception of the idea to the 3D file, this "window frame" is conceived as two different extrusions. It is, one for holding the slide and other to work as "window". This "Window Frame" can be appreciated in the elevation in Figure 4.11.

As explained before in Section 3.5 there are some issues when the thickness of the wall section is thinner than 1 mm. Previous models shown that for a walls thickness of 1 mm or less, the strength could be not enough to support the building process and a extra supports have to be generated manually. In this case, as the $frame$ is only a small part of the whole wall, the necessary supports input manually are reduced to just a few in the middle part of the $frame$. Because of the GAP in the middle of the walls the roof can suffer during the printing process, because of this internal supports have to be added manually but since the inside part of the

test section is accessible through the windows they are not a problem to be removed.

The crystal slide dimensions are $76x26\ mm$. This implies that the first extrusion has to be bigger than those dimensions and the second extrusion has to be smaller so that the slide can be fixed to the frame. Due to these dimensions the model selected to work on is the first model, as its height is very similar with a wall thickness of $2\ mm$ to have space to generate the extrusions. The window frame consist on an extrusion of 1mm with the following dimensions in the YZ plane $27x77\ mm$. This extrusion is not centered but close as possible to the chimney where the droplet will be released. Talking about coordinates in the YZ plane, if the top coordinate of the oil section is fixed in $(15, 0)\ mm$, the chimney is in $(15, 18)\ mm$ and the frame starts in $(17, 14)\ mm$.

The second extrusion makes the slide to be in contact with the inside of the test section, so the camera will be able to film inside of it. In order to avoid problems with the dimensions and to have enough space to paste the slide to the window frame, its dimensions are $0, 5\ mm$ left by each side of the slide, this is, $72x22\ mm$. This "window" unlike the first hole is centered in the previous one so that there is the same spare space by each side of the crystal slide to surround it by glue and be able to avoid leakages.

The process of printing will be almost the same as indicated in previous sections. The only difference is that as there are empty parts on the walls it will be necessary to generate manually supports to the frames. Two models are printed, one with tube connectors for the water and the other without these connections.

As the resin will be used as a support and not to film trough it, the post process after being printed can be with isopropyl since it will not have to be transparent and also the isopropyl will remove all the rests of resin over the printed section.

To handle and manipulate the crystal slide latex gloves are required since they

are very fragile and can get dirty quickly.
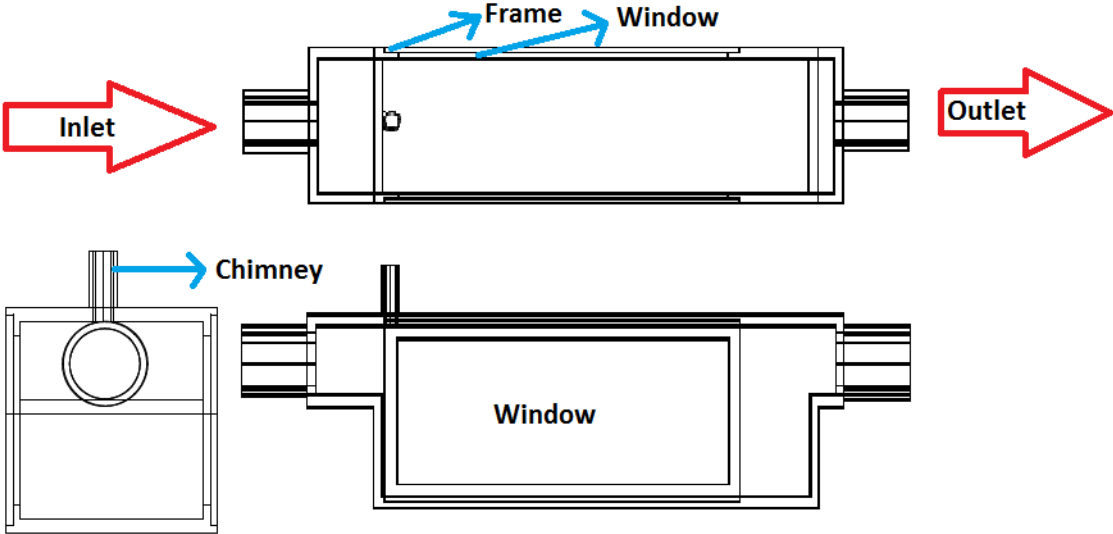

Figure 4.4: Test section planes of the second design without proportions in DWG TrueView 2016 Ⓡ: a) Elevation, b) Plant, c) Profile.

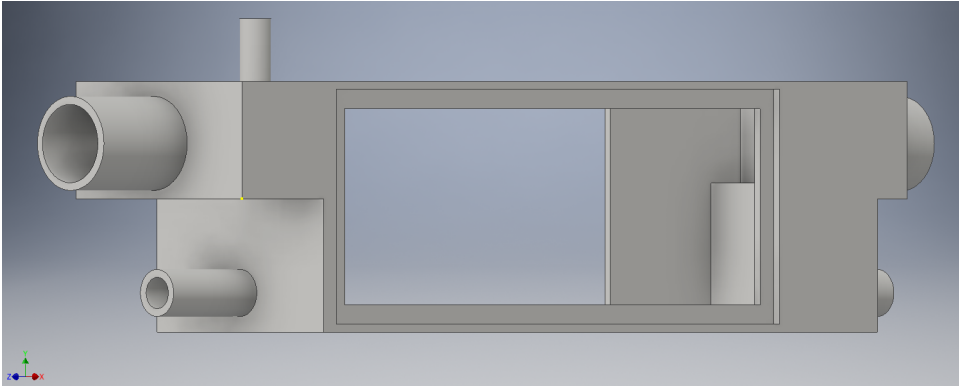

Figure 4.5: Test section model in InventorⓇ.

Final proportions of the re-designed model I is shown below in Table 4.1. The size of the tubes connectors are not included since are kept constant in all the models as it was explained in Chapter 4.

Model	Section	Axes			
		X	Y	Z	Z'
Design I	Oil Section	30	15	600	135
	Water Section	30	20	450	100
	Extrusion I	1	27	-	77
	Extrusion II	1	22	-	72

Table 4.1: Parameters of the test sections.

All the dimensions are in millimeters, Z axis is the real measure and Z' is the scaled one to fit in the printer. The Z dimensions for the extrusions are skipped since it corresponds to models built in a transparent material.

Facility

4.3   Facility set-up

The set-up of the facility was performed in collaboration with the laboratory staff. Reidar was in charge of the mechanical part while Adrien performed the electrical installation. Due to some external factors this set-up lasted four months.

Following the diagram from Figure 3.1 the different components of the system installed are indicated right below and showed in Figures 4.7 and 4.6:

- Flow meter.

- DP cell.

- Flexible pipes.

- Rigid pipes.

- Manual valves.

- 50 L tanks.

- By-pass system.

- Electrical installation.

- Manual control panel.

Figure 4.6: Set-up of the facility.

Figure 4.7: a) Flow meter. b) DP cell. c) Bypass system. d) Pumps installed.

4.4 Instrumentation set-up

After the set-up of the loop components it is needed to install the measurement equipment it counts with. Thorlabs components were used as stands.

- LED lights.

- T-cube LED driver.

- LED stands.

- Syringe stands.

- Camera rail.

- Camera stands.

- Computer.

These items are shown below in Figure 4.12. Camera presented in Figure 4.12 (C)) is the camera that will be used in future experiments but not the one used to perform the illumination set-up as it will be explained later. LEDs stands are adjustable to set different light positions.
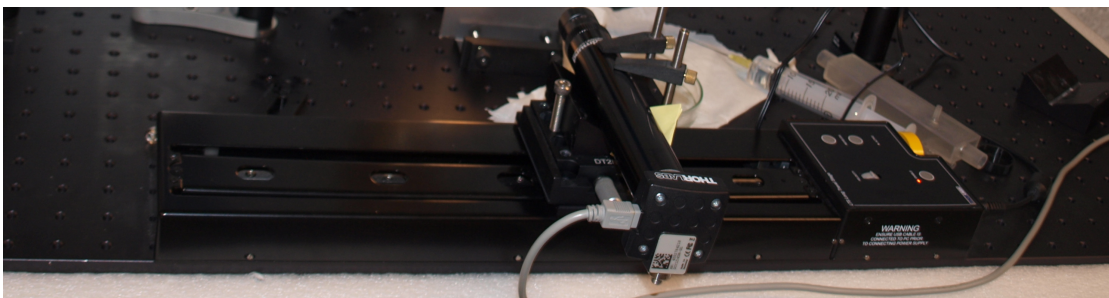

Figure 4.8: Camera rail with DCC1545M-GL camera.

Figure 4.9: a) LEDs stands. b) T-cube LED driver. c) Grasshooper camera. d) Computer.

4.5 Calibration

Due to the height difference of the water between the test section and the flow meter, the water tends to go out through the chimney when high flow rates are used (hydrodynamic jump). Incorporating a flexible pipe section the maximum pump speed found was 50% as whit this speed the height equals the flow meter. Previously in Section 3.3 Figure 3.5 defines the speed and Reynolds number depending on flow rate. For a 50% flow rate (2000 ml/min) flow speed and Reynolds inside the test section are found to be $0, 4$ m/s and $0, 65$ respectively. High speeds also create waves in the entrance of the test section as the flow hits over the entrance ground

Figure 4.10: Control panel.

causing turbulent flow. Anyway, if the pump provides a slow flow (even though the pipes have air inside) the entrance and flow through the test section is valid for illumination tests.

4.6 Visualization and illumination set-up

In this section a practical explanation to find the best illumination in order to be able to record the experiments in the future is presented. This section is an experimental testing of Section 4.4. A DCC1545M-GL Formlabs camera was used to make the set-up of the visualization. To perform the illumination study three different types of LED lights were used behind a diffuser: Green, red and white.

LEDs are controlled manually with T-cube LED drivers. In order to compare results some Exxol droplets where released and filmed with the DCC1545M-GL camera. All
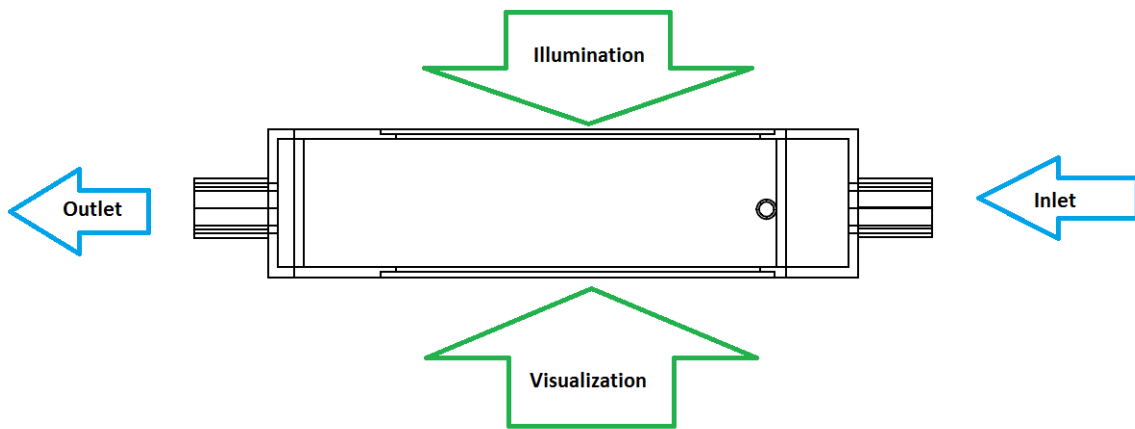
Figure 4.11: Visualization and Illumination sketch.

the illumination set-ups were made with LEDs working at 100% power as it is found for all the colours to provide the most efficient illumination with a diffuser in front of it.

Figure 4.12: a) White LED. b) Green LED.

Green and red LED are both manually adjustable with the two T-cube installed in the facility but white LED is not adjustable so the only thing to do whit it is to regulate its stand to put it far or closer of the diffuser. As the LED light is concentrated in one point, a diffuser is set between LEDs and the back of the test section so that the light can illuminate all the window opened.

The camera is controlled with a free software downloaded in Thorlabs webpage, the ThorCam$^{\text{TM}}$. This camera films in monochrome col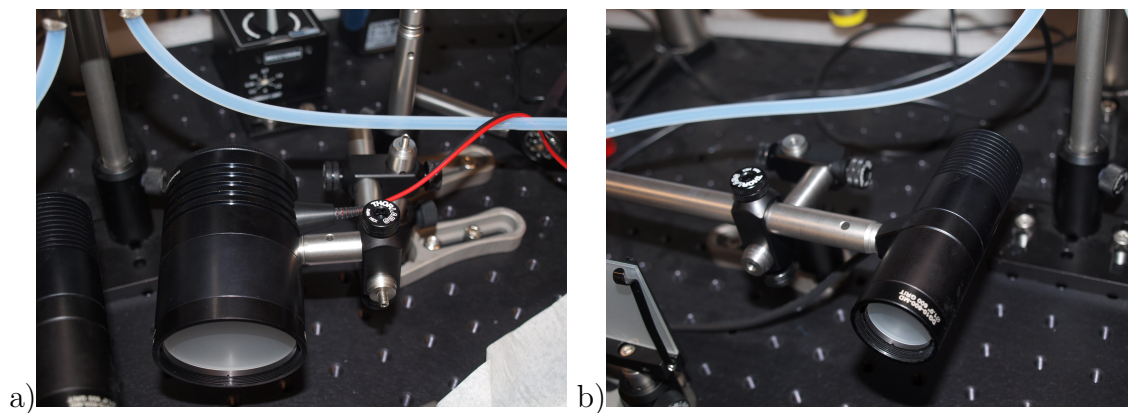our, 1280 x 1024 Pixels at up to 60 Frames per Second. To adjust and focus the camera some Exxsol droplets will be generate manually in static mode of the loop with a water-air interface inside the test section. Two different needle diameters are going to be used:

- **Yellow needle:** $0,7x30\ mm$.

- **White needle:** $1.1x40\ mm$.

The reason why different needles are used is to make sure that the camera can focus it without variate the light set-up.
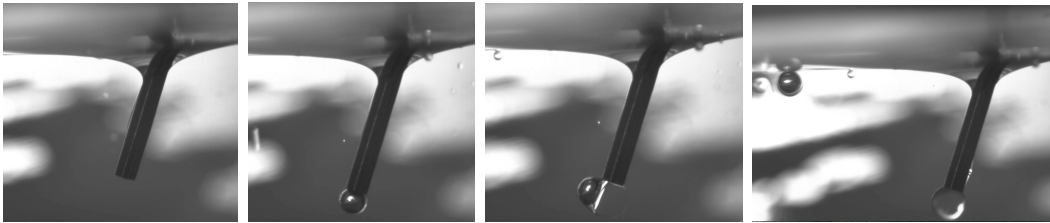

Figure 4.13: Droplet generation with Yellow needle and White LED light. T=2s.
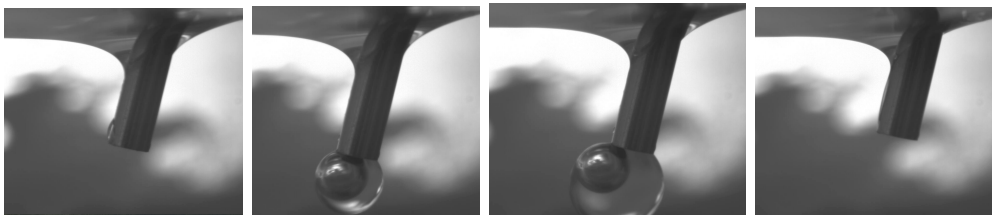

Figure 4.14: Droplet generation with White needle and White LED light. T=1,8s.
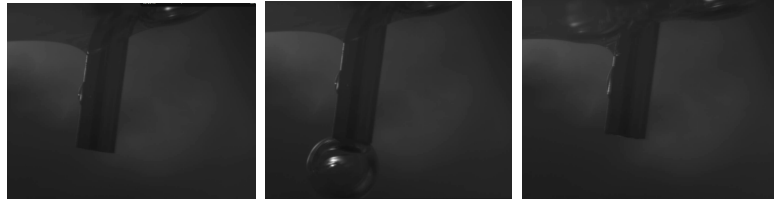
Figure 4.15: Droplet generation with Yellow needle and Red LED light.
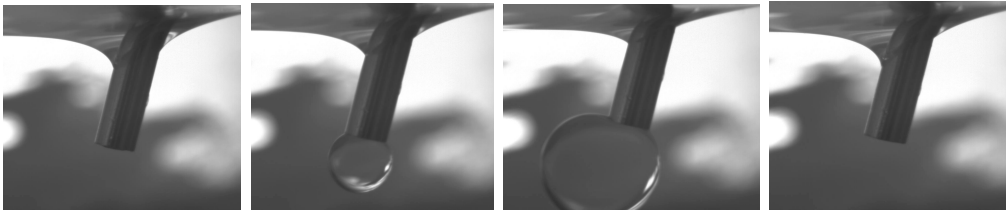
Figure 4.16: Droplet generation with White needle and Green LED light.
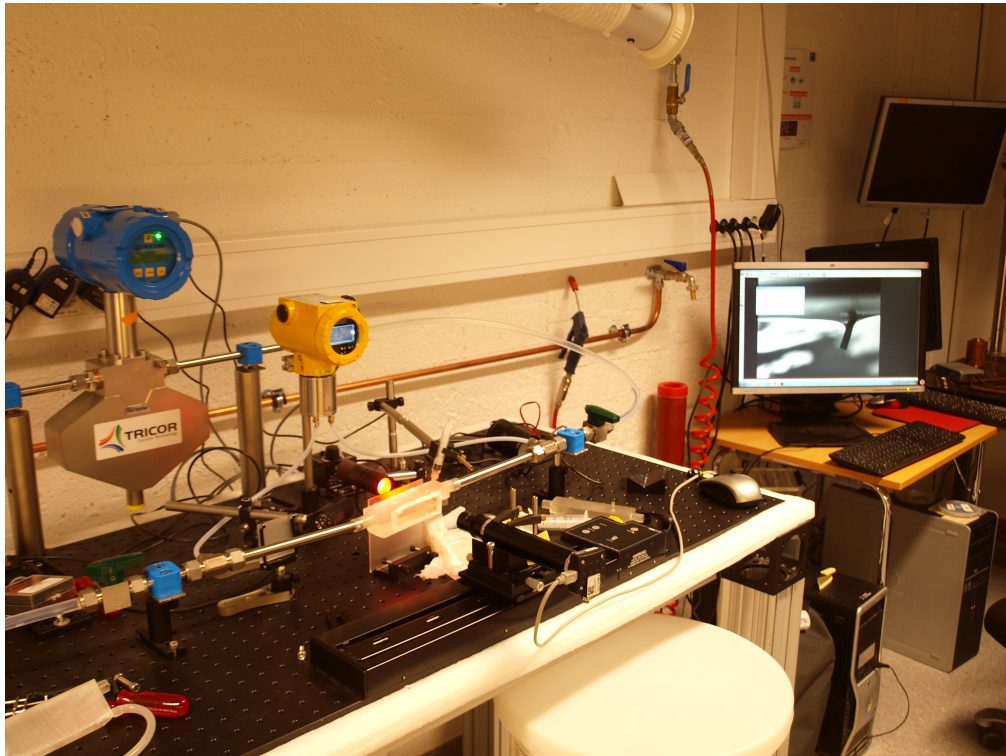
Figure 4.17: Set-up with computer and Red LED.

Chapter 5

Results and discussions

5.1 Test Section

5.1.1 Results

The first model for the test section consisted on a solid piece built in resin. Results of the different post-printing processes applied to the models can be observed in figures from Section 4.1, where the achieved transparency for the later visualization. The best illustration of the different processes is Figure 5.3, where the worst and the best process are confronted. There were no water leakages and the DP indicated a maximum value of $3, 4$ mbar which is an acceptable value for pressure drop in the test section.

5.1.2 Discussion

Although the warm water process could be classified as valid for keeping the grade of transparency of the resin in a very high proportion, the image of the camera is still being disturbed like if the camera lens was unfocused. Even though an infrared camera would be used to film, the shapes will not have to be very visible to be differentiated through the resin walls, the irregular shape in the inside of the walls and the layers do not let to film the coalescence process properly.

Visualization through the resin walls was not an acceptable method to observe the process of gravity separation inside the test section as the resin creates an effect of unfocused in the camera.
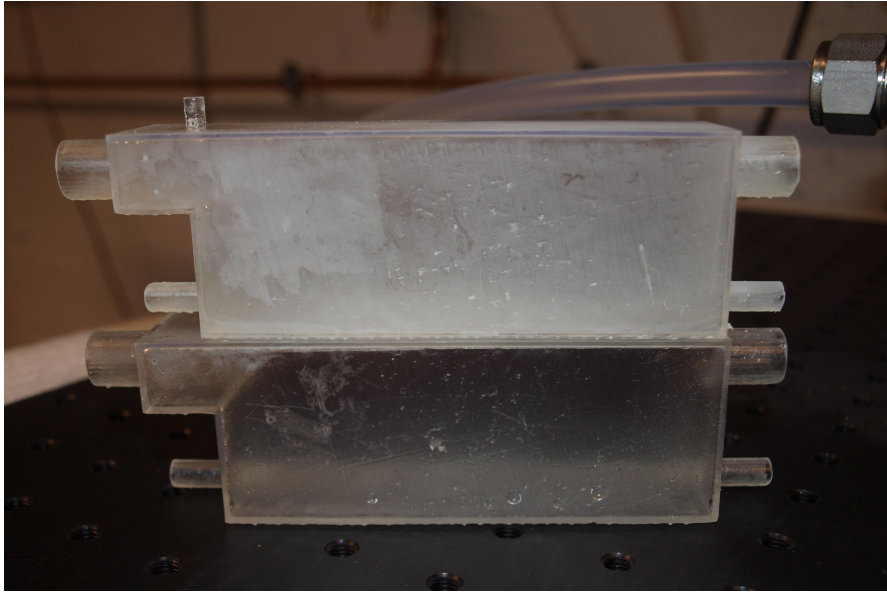
Figure 5.1: Differences between isopropyl process (up) and warm water process (down).

5.2 Test Section Re-design

5.2.1 Results

Second model of the test section was developed in order to achieve the characteristics which first model could not fulfil, this is, transparency for visualization. Second model was designed and built with windows and window frames following Section 4.2. These windows where covered with crystal slides of $76x26$ mm and pasted with plastic silicon as can be appreciated in Figure 5.2. No water leakages where noted after drying of the silicon. DP cell detected a maximum pressure drop of 5 mbar, which as same as the first model is a valid value.
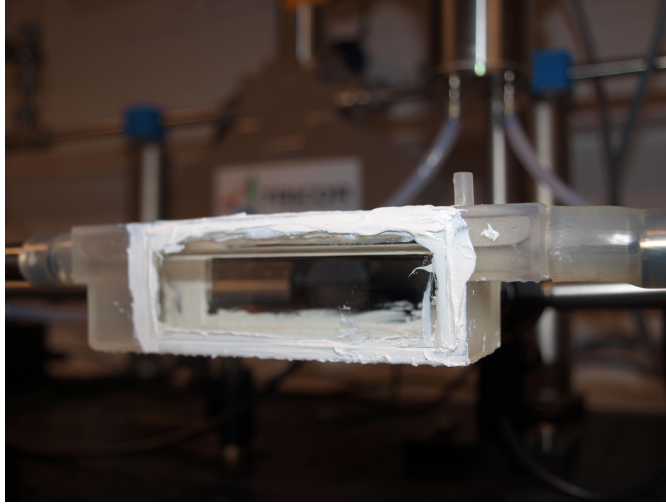
Figure 5.2: Test section with crystal walls and air-water interface.

5.2.2 Discussion

As the printed model has not to provide transparency because of the crystal windows glued, it was not necessary to treat it with a different method than the recommends by the manufacturer These windows allow to observe the inside part of the test section and to illuminate it. Even though the resin was stuck around the test section covering some crystal parts it was not of importance for the visualization process since the interface part was free of silicon as can be observed in Figure 5.2.

5.3 Facility set-up

5.3.1 Results

The loop has been built as is indicated in Section 4.3. Both calibration of the system and visualization process were performed running water from Tank 1 to tank 2 with a maximum speed of 50% of the maximum main pump speed. DP cell was purged and free of water or air droplets and did not appreciated an important pressure drop during the tests. Recirculation pump speed had to be regulated in order to provide

a flow rate which can fill Tank 1 quickly.

Figure 5.3: Close loop of the facility with measuring instrumentation.

5.3.2 Discussion

Some problems were found while running the close loop which has to provide the flow of the lighter liquid on the interface. This problems were related to the different height of the several components facility. The height difference between the Flow meter and the test section creates an hydrodynamic jump which makes the water to look for an exit as it gets into the test section. This is not an important issue since the test section height can be regulated until the Flow meter height. Another solution found would be to change the position of the outlet to a lower one.

5.4 Visualization and Illumination

5.4.1 Results

For visualization and illumination process water was flowed through the loop to create an air water interface inside the test section. Then with the help of an syringe provided with different needle diameter as it has been explained in Section 4.6 Exxsol droplets where released inside the water flow. These droplets were illuminated through a diffuser wall with three different types of LED: white, red and green and filmed with a DCC1545M-GL camera with a Grey scale to black and white. Although in the theory presented in Chapter 2 droplet size is a critical parameter to study the gravity separation process, as this experiment is to validate the illumination and visualization process, the droplet diameter is not important so droplets were made manually.

White LED light is found ti provide the best illumination to visualize the gravity separation process as can be observed in Figure 4.13 and in Figure 4.14.
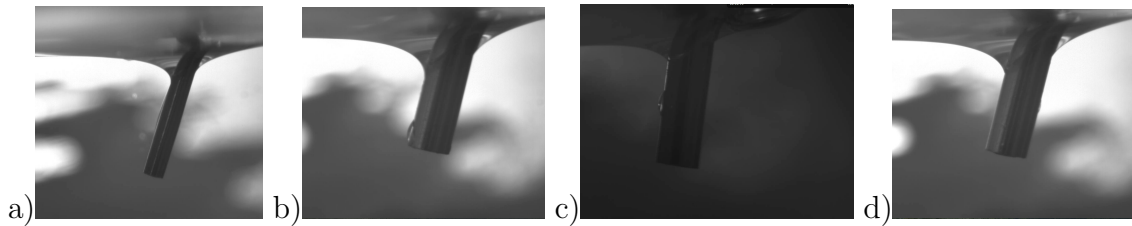
Figure 5.4: a) & b) White LED. c) Red LED. d) Green LED.

5.4.2 Discussion

Some problems are found while using the Exxsol. As its characteristics are quite similar to the water, the droplet formation and its flotation and coalescence on the liquid-liquid interface is almost instantly. Also, some water and air contamination in the Exxsol and in the needle creates some bubbles which affects the Exxsol droplet generation.

As it can be observed above in Figure 5.4 the differences between Green and white illumination is minimum but with the White LED the focus process was easier. This illumination let to film the sedimentation process through the crystal walls and follow it over the camera rail if needed.

Chapter 6

Conclusions and further recommendations

6.1 Conclusions

A test section has been designed and built to reproduce the separation process suffered inside gravity separators. The design has been focused in the influence of the influence of shear over the liquids and over the separation process. The experimental results gotten show that the designed loop and specially the test section cover the demands they were made for and can host the separation process and allow to observe it.

3D printer has been shown as a valid method to manufacture preliminary parts to develop experiments or at least partly since the transparency through different methods have been studied and result were not satisfactory. Resistance of the resin can be insufficient once it gets dried but it allows to check and validate or reject prototypes before spending money, time and resources on it. The aged of the resin has been found to be a critical parameter in the resin properties as it was shown that with the time it was more and more difficult to print a full section.

Illumination and visualization has been presented with a certain grade of succeed.

There are several possible configurations for the illumination with different final effects over the visualization so that depending on the liquids used, as a Grey scale of black and white is used, depending in the different properties between liquids each configuration can be chosen freely.

6.2 Further recommendations

Experimental results show the necessity of a longer test section to let the droplets generated to coalesce inside the test section because of the flow speed. The study of the gravity separation with different flow speeds has to be studied. A printed section build in resin in a 3D printer can be a valid section for small flow rates it would be needed to separate it in several printing sections to later be glued with silicon and a crystal slide would be necessary as a window to be able to observe the inside. It could has problems with the texture of the boards once the silicon dried. Anyway it is highly recommended to build one test section in a transparent material following the dimensions calculated in the theory. Although it can be problematic due to the small pieces needed the final result would be better and more durable.

Concerning the test section design, even though the one presented in this thesis works and has been validates, it is recommended to get low the output of the main liquid flow to avoid problems with hydrodynamic jumps and differences between inlet and outlet flow. It would be also very important to change water inlet and oulet from the XY plane to the XZ, it is, the bottom of the test section and incorporate a separation wall simulating the one present in the gravity separators so the oil has to flood over it as can be observed in Figure 2.3. This wall could help to keep the oil going to Tank 2 free of water and regulate the interface in the test section.

To perform further experiments it will be needed to generate water droplets. This method has to be enough flexible to generate droplets of different diameters and if possible it has to be able to generate clusters so that the influence of neighboring droplets can be studies. In previous thesis student have used electric field pulse

based injection of an electrically neutral water droplet in oil. This method can get droplets of a very small diameter but it can not generate several droplets without being in a queue.

Bibliography

[1] Yining Wu, Taotao Fu, Chunying Zhu, Xiaoda Wang, Youguang Ma, Huai Z. Li. *Shear-induced tail breakup of droplets (bubbles) flowing in a straight microfluidic channel.* Chemical Engineering Science 135, 61-66, 2015.

[2] Taotao Fu, Youguang Ma. *Bubble formation and breeak up dynamics in microfluidic devices: A review* Chemical Engineering Science 135, 343-372, 2015.

[3] S. P. Frankel, K. J. Mysels. *On the dimpling during the approach of two interfaces.* The Journal of Physical Chemistry 66, 190–191, 1962.

[4] S. Hartland and S. A. K. Jeelani. *Choice of model for predicting the dispersion height in liquid/liquid gravity settlers from batch settling data.* Chemical Engineering Science 42 (8), 1927-1938, 1985.

[5] S. A. K. Jeelani and S. Hartland. *Effect of interfacial mobility on thin film drainage.* Journal of Colloid and Interface Science 164, 296–308, 1994.

[6] Siawash Shinwary, Chan Y. Ching and P. Ravi Selvaganapathy. *Monodisperse droplet generation using electrical pulses.* Mcmaster University, Canada, 1522-1524, 2012.

[7] V. Starov, I. Ivanov. *Fluid Mechanics of Surfactant and Polymer Solutions* Springer Vienna, 2014.

[8] *http://formlabs.com/products/3d-printers/form-1-plus/.* Customers service and sel-guide to control the Form 1+ 3D printer.

[9] G. S. Wright, S. Member, P.T. Krein, J.C. Chato and S. Member. *Factors affecting dynamic electrical manipulation of menisci.* IEEE Transaction on Industry Applications 29, 103-112, 1993.

[10] J. Raisin, J. L. Reboud, P. Atten. *Electrocoalescence of water drops in oil shear flow: Development of an experimental set up.* IEEE International Conference on Dielectric Liquids, 2011.

[11] Maurice Stewart and Ken Arnold. *Gas-Liquid And Liquid-Liquid Separators* Burlington, Gulf Professional Publishing, 1 edition, 2008.

[12] Autodesk Inventor info. *http://www.autodesk.com/products/inventor/features/all,* 2016.

[13] J.S.M. Eow, A. Ghadiri,O. Sharif and T.J. Williams. *Electrostatic enhancement of coalescence water droplets in oil: a review of the current understanding.* Chemical Engineering Journal 84 (3), 173-192, 2001.

[14] M. J. H. Simmons, J.A. Wilson, B.J. Azzopardi. *Interpretation of the flow characteristics of a primary oil-water separator from the residence time distribution.* Chemical Engineering Research and Design, Volume 80 (5), 471-481, 2002.

[15] F. Lehr, D. Mewes. *A transport equation for the interfacial area density applied to bubble columns.* Chemical Engineering Science 56, 1159–1166, 1999.

[16] F. Lehr, et al. *Bubble-size distributions and flow fields in bubble columns.*AIChE Journal 48, 2426–2443, 2002.

[17] I. B. Ivanov, D. S. Dimitrov. *Thin Liquid Films.* Dekker, New York, 1988.

[18] T. N. Smith. *A model of settling velocity.* Chemical Engineering Science, 53 (2), 315–323, 1998.

[19] M. A. Waheed, M. Henschke and A. Pfennig. *Simulating sedimentation of liquid drops.* International journal for Numerical Methods in Engineering 59 (14), 1821-1837, 2004.

[20] C. H. Lee et al. *Bubble breakup and coalescence in turbulent gas–liquid dispersions.* Chemical Engineering Communications 59, 65–84. 1987.

[21] W. Rommel, W. Meon, and E. Blass. *Hydrodynamic modeling of droplet coalescence at liquidliquid interfaces.* Separation Science and Technology 27 (2), 129–159, 1992.

[22] Ahmed H. Abdel-Alim and A. E. Hamielec. *A Theoretical and Experimental Investigation of the Effect of Internal Circulation on the Drag of Spherical Droplets Falling at Terminal Velocity in Liquid Media.* Ind. Eng. Chem. Fundamen. 14 (4), 308–312, 1975.

[23] Panagiota Angeli, Geoffrey F. Hewitt. *Drop size distributions in horizontal oil-water dispersed flow.* Chemical Engineering Scicence 55, 3133-3143, 2000.

[24] R. C. Chen and J. L. Wu. *The ow characteristics between two interactive spheres.* Chemical Engineering Science 55, 1143–1158, 2000.

[25] B. V. Derjaguin, M. M. Kussakov. *Anomalous properties of thin polymolecular films.* Acta Physicochim. URSS, 10, 25–30, 1939.

[26] *Specifications for oil and gas separators.* American Petroleum Institute, Production Department, 1989.

[27] M. J. H. Simmons, B. J. Azzopardi. *Drop size distributions in dispersed liquid-liquid pipe flow.* International Journal of Multiphase Flow 27, 843-859, 2000.

[28] J. Lovick, P. Angeli. *Droplet size and velocity profiles in liquid-liquid horizontal flows.* Chemical Engineering Scicence 59, 3105-3115, 2004.

[29] J. Tallero, Cem Sarica, J.P. Brill. *A study of oil/water flow patterns in horizontal pipes* Society of Petroleum Engineers 12 (3), University of Tulsa, 1997.

[30] A. Kumar. *Droplet behaviour in liquid-liquid extraction.* Swiss Federal Institute of Technology, Zurich, 1983.

[31] J. Lovick, P. Angeli. *Experimental studies on the dual continuous flow pattern in oil-water flows.* International Journal of Multiphase Flow 30, 139-157, 2004.

[32] P. C. Duineveld. *Bouncing and coalescence of two bubbles in water.* Ph.D. Dissertation, University of Twente, The Netherlands, 1994.

[33] L. Doubliez. *The drainage and rupture of a non-foaming liquid film formed upon bubble impact with a free surface.* International Journal of Multiphase Flow 17, 783–803, 1991.

[34] G. B. Jeffery. *The motion of ellipsoidal particles immersed in a viscous fluid.* Proc. Roy. SOCA, 102-161, 1922.

[35] M. Mousavichoubeh, M. Shariaty-Niassar, and M. Ghadiri. *The effect of interfacial tension on secondary drop formation in electro-coalescence of water droplets in oil.* Chemical Engineering Science 66, 5330–5337, 2011.

[36] E.C. Eckstein, D. G. Bailey A. H. Shapiro. *Self-diffusion of particles in shear flow of a suspension.* J. Fluid Mech. 79 (1). 191-208, 1977.

[37] A. Karnish,H. L. Goldsmith and S. G. Mansons. *The kinetic of flowing dispersions; I. Concentrated suspensions of rigid particles.* J . Colloid Interface Sci. 22, 531, 1966a

[38] G. E. Charles and S. G. Mason. *The coalescence of liquid drops with at liquid/liquid interface* Journal of Colloid Science 15(3), 236–267, 1960.

[39] J. Happel and H. Brenner. *Low Reynolds Number Hydrodynamics: With Special Applications to Particulate Media.* Martinus Nijhoff Publishers, 1 edition, 1983.

[40] T. D. Hodgson, J. C. Lee. *The effect of surfactants on the coalescence of a drop at an interface. i.* Journal of Colloid and Interface Science, 30(1), 94–108, 1969.

[41] M. Simon. *Koaleszenz von Tropfen und Tropfenschwärmen* Ph.D.Disserta- tion, dieTeschinschenUniverstität Kaiserslautern, 2004.

[42] Xiao-Xuan Xu. *Study on oil-water two-phase flow in horizontal pipes.*Journal of Petroleum Science and Engineering 59, 43-58, 2007.

[43] C. T. Chen, J. R. Maa, Y. M. Yang, and C. H. Chang. *Effects of electrolytes and polarity of organic liqiuds on the coalescene of droplets at aqueous-organic interfaces.* Surface Science 406, 167– 177, 1998.

[44] O. M. H Rodriguez, R. V. A. Oliemans. *Experimental study on oil-water flow in horizontal and slighty inclined pipes.* International Journal of Multiphase Flow 32, 323-343, 2006.

[45] P. Angeli, G. F. Hewitt. *Flow structure in horizontal oil-water flow.* International Journal of Multiphase Flow 26, 1117-1140, 2000.

[46]] M. Saeid, A. P. William, and G. S. James. *Handbook of Natural Gas Transmission and Processing, Chapter 5 – Phase Separation.* Burlington, Gulf Professional Publishing, 2006.

[47] T. Frising, C. Noïk, and C. Dalmazzone. *The Liquid/Liquid Sedimentation Process: From Droplet Coalescence to Technologically Enhanced Water/Oil Emulsion Gravity Separators: A Review.* Journal of Dispersion Science and Technology, 27, 1035–1057, 2006.

[48] Y. Liao and D. Lucas. *A literature review on mechanisms and models for the coalescence process of fluid particles.* Chemical Engineering Science 65, 2851–2864, 2010.

[49] Pieter De Bruyn, Ruth Cardinaels, Paula Moldenaers. *The effect of geometrical confinements on coalescece efficiency of droplet pairs in shear flow.* Journal of Colloid and Interface Science 409, 183-192, 2013.

[50] S. Hartland and S. A. K. Jeelani. *Prediction of sedimentation and coalescence profiles in a decaying batch dispersion.* Chemical Engineering Science 4 (9), 2421-2429, 1988.

[51] J. Raisin, J. L. Reboud and P. Atten. *Electrocoalescence of water drops in oil shear flow: Development of an experimental set up.* IEEE International Conference on Dielectric Liquids, 2011.

[52] Z.-G. Feng and E. E. Michaelides. *Drag coecients of viscous spheres at intermediate and high reynolds numbers.* Journal of Fluids Engineering 123, 841–849, 2001.

[53] D. li. *Coalescence between two small bubbles or drops.* Journal of Colloid and Interface Science 163, 108–119, 1994.

[54] M. Jalaal, B. Khorshidi, E. Esmaeilzadeh. *An experimental study on the motion, deformation and electrical charging of water drops falling in oil in the presence of high voltage D.C. electric field.* Experimental Thermal and Fluid Science 34, 1498–1506, 2010.

[55] J. H. Perry. *Perry Chemical Engineers' Handbook.* New York, McGraw-Hill Publishing CompanyLtd., 1950.

[56] J. C. Lee, T. D. Hodgson. *Film Flow and Coalescence-I Basic relations film shape and criteria for interface mobility.* Chemical Engineering Science 23, 1375-1397, 1968.

[57] R. Clift, J. R. Grace and M. E. Weber. *Bubbles, drops and particles.* Academic Press Inc, 1978.

[58] E. Loth. *Quasi-steady shape and drag of deformable bubbles and drops.* International Journal of Multiphase Flow, 34, 523–546, 2008.

[59] S. C. Liang, T. Hong and L. S. Fan. *Effects of particle arrangements on the drag force of a particle in the intermediate flow regime.* International Journal of Multiphase Flow, 22 (2), 285–306, 1996.

[60] S. B. Lang and C. R. Wilke. *A Hydrodynamic Mechanism for the Coalescence of Liquid Drops. I. Theory of Coalescence at a Planar Interface.* Industrial & Engineering Chemistry Fundamental 10 (3), 329-340, 1960(a).

[61] S. B. Lang and C. R. Wilke. *A Hydrodynamic Mechanism for the Coalescence of Liquid Drops. II. Experimental studies.* Industrial & Engineering Chemistry Fundamental 10 (3), 341-352, 1960 (b).

[62] O. Reynolds. *On the theory of lubrication and its application to mr. beauchamp tower's experiments, including an experimental determination of the viscosity of olive oil.* Philosophical Transactions of the Royal Society of London 177, 157–234, 1986.

[63] M. Chiesa, J. A. Melheim, A. Pedersen, S. Ingebrigtsen, and G. Berg. *Forces acting on water droplets falling in oil under the influence of an electric field: Numerical predicitons versus experimental observations.* European Journal of Mechanics B/Fluids 24, 717–732, 2005.

[64] W. L. Haberman and R. M. Sayre. *Motion of rigid and uid spheres in stationary and moving liquids inside cylindrical tubes.* David W. Taylor Model Basin Report No. 1143. Washington, DC, 1958.

[65] K. D. Danov. *Effect of Surfactants on Drop Stability and Thin Film Drainage.* Fluid Mechanics of Surfactant and Polymer Solutions (CISM Courses and Lectures 463), 1–38, 2004.

[66] M. Loewenberg, E. J. Hinch. *Collision of two deformable drops in shear flow.* J. Fluid Mech. 338, 299-315, 1997.

[67] Elka S. Basheva, Theodor D. Gurkov, Ivan B. Ivanov, Grigor B. Bantchev, Bruce Campbell, Rajendra P. Borwankar. *Size Dependence of the Stability of Emulsion Drops Pressed against a Large Interface.* Langmuir 15, 6764-6769, 1999.

[68] S. A. K. Jeelani and S. Hartland. *Effect of surface mobility on collision of spherical drops.* Journal of Colloid and Interface Science 206, 83–93, 1998.

[69] A. K. Chesters. The applicability of dynamic-similarity criteria to isothermal, liquid–gas, two-phase flows without mass-transfer. International Journal of Multiphase Flow 2, 191–212, 1975.

[70] S. A. K. Jeelani and S. Hartland. The continuous separation of liquid/liquid dispersions Chemical Engineering Science 48 (2), 239–254, 1993.

[71] A. K. Chesters. *The modelling of coalescence processes in uid-liquid dispersions: A review of the current understanding.* Chemical Engineering Research and Design 69A, 259–269, 1991.

[72] M. Dhainaut. *Literature Study on Observations and Experiments on Coalescence and Breakup od Bubbles and Drops.* SINTEF report, 3-25.

[73] F. Da Cunha, E. Hinch. *Shear-induced dispersion in a dilute suspension of rough spheres* J. Fluid Mech. 309, 211-233, 1996.

[74] J. M. H. Janssen and H. E. H. Meijer.*Droplet reakup mechanisms:Stepwise equilibrium versus transient dispersion.* Journal of Rheology 37(4), 597608, 1993.

[75] Nicholas N. A. Ling, Agnes Haber, Einar O. Fridjonsson, Eric F. May, Michael L. Johns. *Shear-induced emulsion droplet diffusion studies using NMR.* Journal of Colloid and Interface Science 464, 229-237, 2016.